Reconstruction of the complete human cytomegalovirus genome in a BAC reveals RL13 to be a potent inhibitor of replication

Richard J. Stanton,[1] Katarina Baluchova,[2] Derrick J. Dargan,[2] Charles Cunningham,[2] Orla Sheehy,[2] Sepehr Seirafian,[1] Brian P. McSharry,[1] M. Lynne Neale,[1] James A. Davies,[1] Peter Tomasec,[1] Andrew J. Davison,[2] and Gavin W.G. Wilkinson[1]

[1]Section of Medical Microbiology, Tenovus Building, School of Medicine, Cardiff University, Cardiff, United Kingdom. [2]MRC Virology Unit, Institute of Virology, University of Glasgow, Church Street, Glasgow, United Kingdom.

Human cytomegalovirus (HCMV) in clinical material cannot replicate efficiently in vitro until it has adapted by mutation. Consequently, wild-type HCMV differ fundamentally from the passaged strains used for research. To generate a genetically intact source of HCMV, we cloned strain Merlin into a self-excising BAC. The Merlin BAC clone had mutations in the RL13 gene and UL128 locus that were acquired during limited replication in vitro prior to cloning. The complete wild-type HCMV gene complement was reconstructed by reference to the original clinical sample. Characterization of viruses generated from repaired BACs revealed that RL13 efficiently repressed HCMV replication in multiple cell types; moreover, RL13 mutants rapidly and reproducibly emerged in transfectants. Virus also acquired mutations in genes UL128, UL130, or UL131A, which inhibited virus growth specifically in fibroblast cells in wild-type form. We further report that RL13 encodes a highly glycosylated virion envelope protein and thus has the potential to modulate tropism. To overcome rapid emergence of mutations in genetically intact HCMV, we developed a system in which RL13 and UL131A were conditionally repressed during virus propagation. This technological advance now permits studies to be undertaken with a clonal, characterized HCMV strain containing the complete wild-type gene complement and promises to enhance the clinical relevance of fundamental research on HCMV.

Introduction

Human cytomegalovirus (HCMV) is a clinically important herpesvirus that is ubiquitous in human populations worldwide (1). Primary infection is followed by lifelong persistence, during which virus reactivation must be constrained continuously by host immune surveillance. Myeloid cell progenitors are a recognized site of latency, with infectious virus being produced following differentiation into macrophages or dendritic cells. Severe disease is most commonly observed when immunity is compromised by infection (e.g., HIV/AIDS) or immunosuppressive therapy (e.g., in transplant recipients). HCMV is also the leading viral cause of congenital disability and malformation, which was the primary basis for it being designated a highest priority level vaccine target by the US Institute of Medicine (2). HCMV disease can manifest as a wide range of clinical conditions (e.g., pneumonia, colitis, retinitis, hepatitis, arteriosclerosis, or systemic infection), reflecting the capacity of the virus to infect a wide range of cell types in vivo (3–7). Despite this wide tropism in vivo, only fibroblasts support the efficient growth of cultured strains in vitro.

Appreciation of HCMV pathogenesis is heavily dependent on research performed using the high-passage strains AD169 and Towne. However, these strains are known to have both lost virulence and experienced substantial alterations in their genomes during passage in cell culture (8–10). The HCMV genome may be represented as *ab*-U_L-*b′a′c′*-U_S-*ca*, where U_L and U_S denote long and short unique regions and *ba*/*b′a′* and *ca*/*c′a′* indicate inverted repeats flanking the unique regions. AD169 and Towne have acquired large deletions (15 kb and 13 kb, respectively) in the U_L/*b′* region in addition to defects elsewhere in genes that are dispensable for growth in fibroblasts (11–18). The U_L/*b′* region encodes a viral CXCL chemokine (gene UL146; ref. 19), a tumor necrosis factor receptor homolog (gene UL144; ref. 20), natural killer cell evasion functions (genes UL141 and UL142; refs. 21–23), a regulator of latency (gene UL138; refs. 24, 25), and several other uncharacterized functions. Therefore, the U_L/*b′* region is likely to contribute to virulence via several pathways. Spontaneous defects clearly arise elsewhere in the HCMV genome, yet their significance is only occasionally defined functionally (13, 18, 26, 27). Indeed, whole-genome sequencing of multiple clinical strains following growth in vitro reveals that clinical HCMV genomes invariably mutate whether passaged in fibroblasts, epithelial cells, or endothelial cells (28).

There is a need to develop and characterize low-passage HCMV strains for experimental applications. However, the generation of laboratory strains of WT HCMV is problematic not only because clinical samples often contain multiple strains (27, 29–36), but especially because genetic adaptations occur even during the early stages of passage in cell culture. Thus, most strains passaged in fibroblasts are mutated in 1 of 3 adjacent genes (UL128, UL130, and UL131A; collectively termed the UL128 locus, UL128L) whose products form a complex bound to glycoproteins gH and gL in the virion envelope (37–43). These mutations inhibit formation of the complex and thereby render the virus incapable of infecting epithelial, endothelial, and certain myeloid cell types (12, 44–48).

Authorship note: Richard J. Stanton and Katarina Baluchova contributed equally to this work.

Conflict of interest: The authors have declared that no conflict of interest exists.

Citation for this article: *J Clin Invest.* 2010;120(9):3191–3208. doi:10.1172/JCI42955.

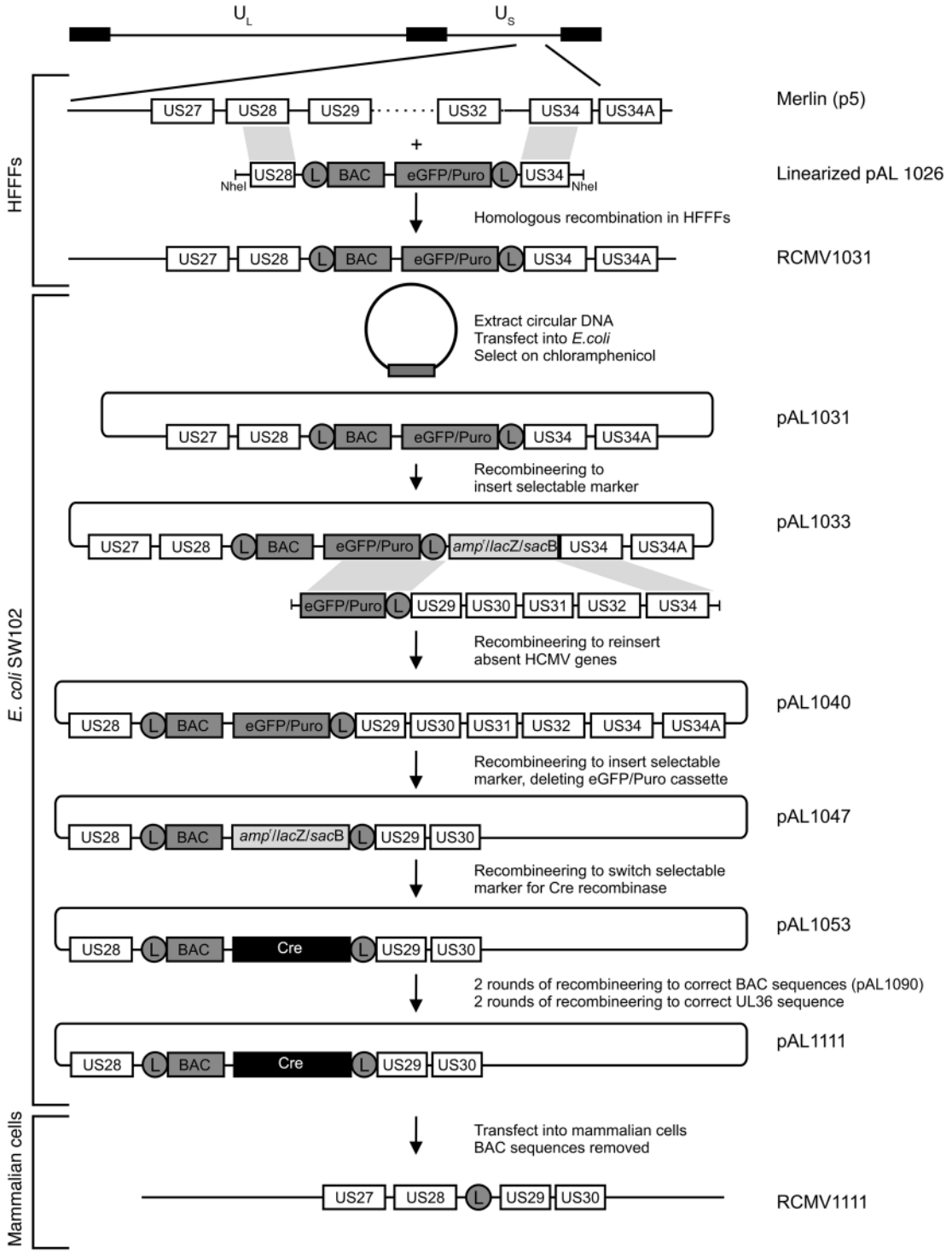

Figure 1
Steps in the construction of pAL1111. The approximate location of the insertion site of the BAC vector between US28 and US29 in the U_S region of the HCMV genome is shown at the top. The designations of BACs (pAL series) and viruses (RCMV series) are shown on the right. Boxes indicate protein-coding regions (labeled), and circles denote *loxP* sites (L). The BAC box represents pBeloBAC11, the eGFP/Puro box represents a cassette expressing eGFP and a puromycin resistance protein, and the Cre box represents a Cre recombinase gene containing a synthetic intron.

Table 1
Sequence differences between Merlin (NC_006273) and the HCMV genome in pAL1053

Position	Change (NC_006273 → pAL1053)	Coding region affected	Coding effect
11363	CAAAAAAAC → CAAAAAAAAC	RL13	*f*
40231	TTGGAGG → TTGCAGG	UL32	None
48828	GGCGAAC → GGCAAAC	UL36	R → C
49054	CATGATC → CATCATC	UL36	I → M
49203	GACGGTA → GACAGTA	UL36	R → C
49791	AGGGGTG → AGGAGTG	UL36	*P* → S
49792	GGGGTGC → GGGCTGC	UL36	H → Q
194592–194643 (1025–1076)	ACACCCCCCGTCCCCGCACACCCCCCGTCCCCGCACACCCCCCGTCCCCG → G	None (*b*/*b*′)	None
195063 (605)	GGACCGC → GGAGCGC	None (*b*/*b*′)	None
194781	CCGTAGA → CCGCAGA	None (*b*′ only)	None

Nt positions are given with respect to NC_006273. *f*, frameshift. Altered bases underlined.

The genomes of several HCMV strains have been captured as BACs, including a number based on low-passage viruses, and these are proving to be an invaluable resource for research (49–54). However, none contains the full complement of HCMV genes, both because of mutations that occurred in cell culture prior to being cloned and, in most cases, because sequences were deleted in order to accommodate the BAC vector. In addition, the original clinical material is not available for most of these strains, thus preventing the sequences of the cloned genomes being verified against those of unpassaged virus. To provide a reliable source of HCMV gene sequences and a reproducible source of genetically intact, clonal virus for pathogenesis studies, we sought to produce an infectious BAC containing the complete HCMV gene complement. HCMV strain Merlin (ATCC VR-1590) was selected because it is designated the reference HCMV genome sequence by the National Center for Biotechnology Information (GenBank AY446894; RefSeq NC_006273) and the original clinical sample is available for comparison. Merlin was derived from the urine of a congenitally infected infant and sequenced after 3 passages (p3) in human fibroblasts (27).

Our study commenced with the construction of a BAC clone containing the complete genome of strain Merlin (p5). DNA sequencing led to the identification of disabling mutations in genes RL13 and UL128, which were repaired first singly and then in combination to produce BACs containing a complete WT gene complement. Experiments conducted with viruses derived from the BACs revealed that RL13 expression severely impairs HCMV replication in fibroblast and epithelial cell cultures. Thus, when viruses generated from BACs containing the WT RL13 gene were passaged in vitro, further mutants emerged rapidly, producing a phenotypically altered virus with enhanced growth properties. Although RL13 is known to be a member of a restricted set of HCMV hypervariable genes (27), its expression had not, to our knowledge, previously been characterized. Use of the BACs showed that RL13 encodes a highly glycosylated protein located in the virion envelope. Since virus generated from the WT BAC was susceptible to mutation, cell lines were constructed in which expression of RL13 and UL131A could be modulated. For what we believe is the first time, these cell lines permit experiments to be undertaken using a characterized HCMV strain containing the complete WT gene complement.

Results

Cloning the HCMV strain Merlin genome. We aimed to clone the complete HCMV strain Merlin genome by inserting a BAC vector into a noncoding region between virus genes US28 and US29. Preliminary studies (data not shown) indicated that straightforward insertion of the BAC-targeting vector into the HCMV genome by homologous recombination during virus growth in primary human fetal foreskin fibroblasts (HFFFs) was associated with compensating deletions in virus sequences, presumably due to genome size constraints operating during virus DNA packaging. The BAC-targeting vector was therefore redesigned to replace the region of the HCMV genome containing US29–US34 (Figure 1). BAC vector DNA was transfected into HFFFs, which were superinfected with HCMV strain Merlin (p5), and puromycin selection was used to enrich for recombinants. Circular DNA was extracted and electroporated into *E. coli*. A total of 22 clones were analyzed by restriction endonuclease digestion (data not shown), and all contained the HCMV genome minus US29–US34. Since both U_L and U_S may be present in either orientation in an HCMV genome, a linear molecule will be one of 4 isomers and a circular molecule one of 2. Restriction endonuclease profiles corresponding to both circular conformations were detected among the BAC clones (data not shown). A single clone (pAL1031; Figure 1) of the 12 clones with U_L and U_S present in the standard arrangement was selected for further analysis.

Recombineering (55, 56) was used to insert the US29–US34 region into pAL1031, thus generating pAL1040, which contains the entire Merlin genome (Figure 1). Cre/lox technology has been deployed previously to promote excision of prokaryotic vector sequences (also located between US28 and US29) from an AD169 BAC following transfection into HFFFs (53). We adopted this strategy to produce a self-excising Merlin BAC by 2 rounds of recombineering, in which the enhanced GFP (eGFP)/Puro cassette in pAL1040 was replaced by a gene encoding Cre recombinase, thus generating pAL1053 (Figure 1). The version of Cre used contained a synthetic intron to prevent its expression in *E. coli* (57, 58). Following transfection into HFFFs however, Cre recombinase was expressed and mediated removal of the BAC vector by recombination between *loxP* sites engineered at the junctions with the virus genome. Thus, the only exogenous sequences remaining in virus generated from pAL1053 and subsequent BACs were those of single *loxP* and NheI sites (40 bp in total) located between US28 and US29 (Figure 1).

Sequence of BAC pAL1053. Sequencing of the entire HCMV component of pAL1053 confirmed that the whole Merlin genome had been captured and that a single *a*/*a*′ sequence was present between

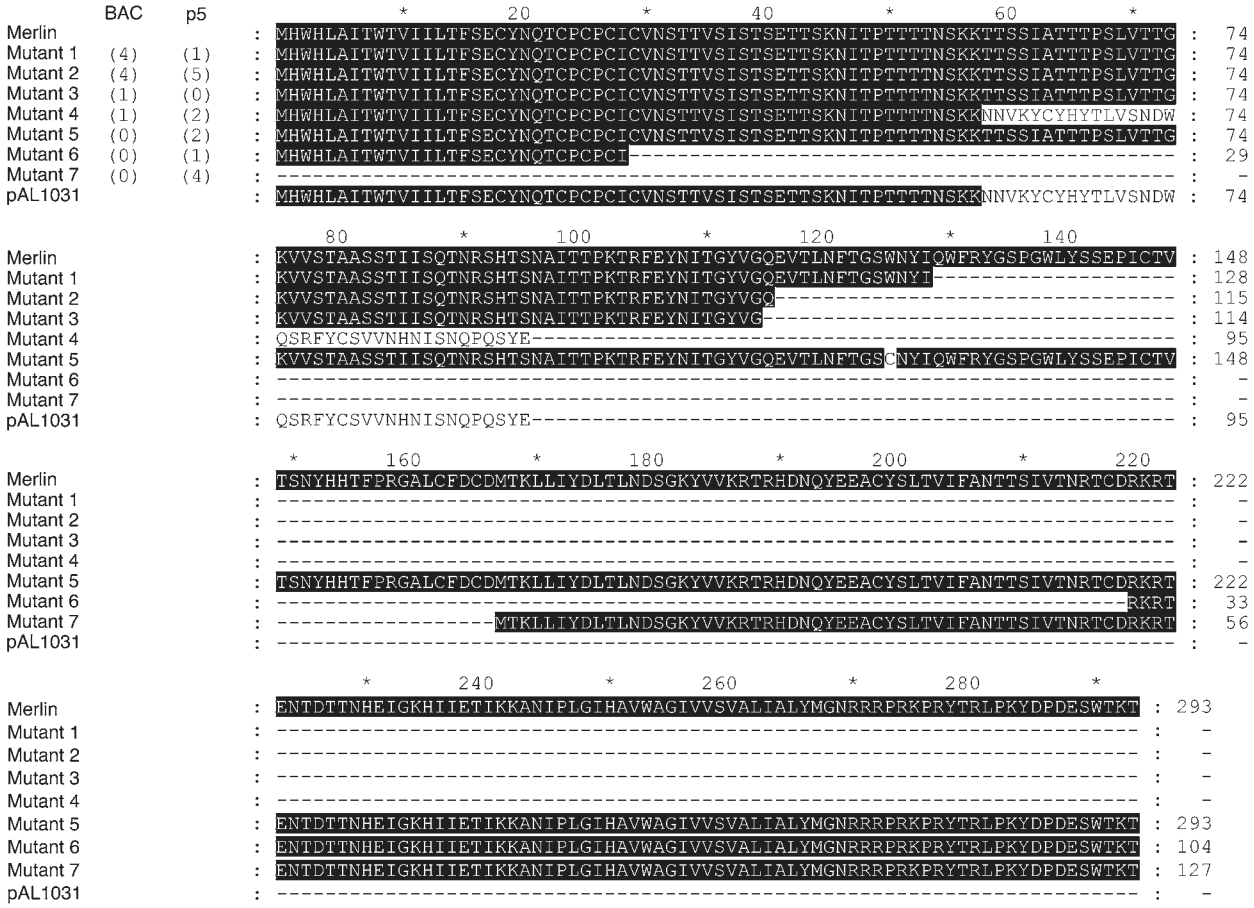

Figure 2

Alignment of amino acid sequences potentially encoded by mutated versions of RL13 in pAL1031 and 10 other BACs from this stage, and PCR clones from Merlin (p5). Shading indicates identity to the WT Merlin sequence (NC_006273). Numbers in parentheses indicate the number of clones containing the relevant mutation. Nt mutations were as follows (numbering relative to strain Merlin sequence, NC_006273): mutant 1, C → T (nt 11573; premature stop codon); mutant 2, G → T (nt 11534; premature stop codon); mutant 3, C → T (nt 11531; premature stop codon); mutant 4 (which includes pAL1031), extra A (nt 11363; frameshift); mutant 5, G → C (nt 11563, W → C); mutant 6, deletion of nt 11276–11860; mutant 7, G → A (nt 11191, M → I, altered start codon; the protein is depicted as starting from next in-frame M).

the *b* and *c*, and *b′* and *c′*, sequences. As in Merlin (p3), pAL1053 contained a G to A (G → A) substitution at nt 176311 that introduces an in-frame stop codon and would lead to premature termination of the UL128 protein. pAL1053 differed from Merlin (p3) at a total of 12 locations (Table 1). These included 5 substitutions clustered in UL36. The sequences of PCR products amplified from the original clinical material, Merlin (p3), the earliest BAC precursor of pAL1053 (pAL1031), and 10 additional Merlin BACs from the same stage as pAL1031 showed that these mutations were present only in pAL1031, whereas the sequences from all other sources were identical to that of the Merlin (p3) sequence. Thus, the differences in UL36 were atypical and limited to the Merlin genome that was captured in pAL1031. The UL36 mutations in pAL1053 were repaired by recombineering to match the Merlin (p3) sequence, thus generating pAL1111 (Figure 1).

The most significant additional difference between Merlin (p3) and pAL1053 (and hence pAL1111) was a frameshift in RL13 at nt 11363 caused by a single nt insertion (Table 1; also see below). The remaining differences had no apparent effect on protein-coding potential. A synonymous substitution in gene UL32 was found retrospectively to represent a single nt polymorphism in the Merlin (p3) genome. Three alterations were noted in the *b*/*b′* inverted repeat sequence. Two of these were substitutions, one being present in both *b* and *b′* and the other in *b′* alone. The other was a 51-bp deletion due to natural length variation in a tandem repeat sequence in both *b* and *b′*. The *b*/*b′* sequence is the region of the HCMV genome that is most prone to variation in HCMV (18, 59)

Mutations in RL13. To investigate the origin of the frameshift mutation in the RL13 coding region (nt 11189–12070), this locus was sequenced in 10 additional BACs from the same stage as pAL1031. Surprisingly, all were found to contain disruptive mutations, and 4 different classes (classes 1–4) of mutant were identified, each of which is predicted to express a truncated RL13 protein (Figure 2). To determine whether RL13 was mutated in the virus stock used to generate pAL1031, the coding region was amplified by PCR from Merlin (p5) and 15 clones were sequenced (Figure 2). Mutations that were detected in single clones, except where they corresponded to mutations in the BACs, could have arisen by PCR error and were excluded from the analysis. The PCR clones identified mutations that corresponded to 3 of the 4 mutant groups

Table 2
Sequence differences between RL13 in WT Merlin (NC_006273) and subpopulations of Merlin (p3) represented in bacteriophage M13 or PCR clones

Position	Mutation (NC_006273 → clone)	Residue	Coding effect	No. of M13 clones	No. of PCR clones
11191	CATGCAC → CATACAC	1	M → I	1/6	0/22
11537	GAAGTGA → GAAATGA	117	V → M	4/8	11/22
11563	ATGGAAT → ATGCAAT	125	W → C	2/8	1/22
11563	ATGGAAT → ATGCAAT	125	W → C	2/8	4/22
11900	ATTGAAA → ATTCAAA	238	E → Q	2/8	4/22
11884	AATCGGG → AATTGGG	232	None	1/8	2/22
11964	TATCGGT → TATAGGT	259	S → X	1/8	2/22

Nt positions are given with respect to NC_006273. X, termination codon. Altered bases underlined.

(groups 1, 2, and 4) in BACs, plus 3 additional groups (classes 5–7). None of the BAC or PCR clones yielded a sequence representing the WT RL13 coding region.

The finding that all genomes in Merlin (p5) and BACs derived from Merlin at the pAL1031 stage were mutated in RL13 raised the question of at which stage these mutations had arisen. The original Merlin sequence was determined from bacteriophage M13 clones derived from Merlin (p3). Retrospective analysis of the sequence database revealed that, although the RL13 consensus was WT, all individual M13 clones were mutated at various different positions (Table 2). Moreover, an analysis of individual PCR clones produced from Merlin (p3) was also consistent with this virus stock comprising a mixture of RL13 mutants (Table 2). Thus, 18/22 PCR clones exhibited substitutions that were also detected in the M13 clones. Each of the remaining 4/22 PCR clones contained unique mutations in RL13 (data not shown), though it is not possible to exclude the possibility that these resulted from PCR errors.

To investigate whether the mutants detected in Merlin (p3 and p5) were present in the clinical sample or whether they originated during cell culture, 10 PCR clones of RL13 were generated from the original clinical sample, using the same primers and conditions as were used for Merlin (p5). Nine clones were WT in sequence, and one clone contained a single synonymous substitution (A → G at nt 11959). This substitution was not detected in any versions of Merlin from passage in cell culture and thus most probably resulted from a PCR error. These data indicated that RL13 was predominantly WT in the clinical sample and are consistent with RL13 mutants having arisen and been selected during cell culture.

Growth properties of virus generated from the Merlin BAC. Virus (RCMV1111) was readily recovered from HFFFs transfected with pAL1111 (Figure 1) and exhibited a restriction endonuclease profile identical to that of Merlin (p5) (Figure 3A). A pattern diagnostic of the presence of all 4 genome isoforms was distinguishable in the linear RCMV1111 genome. Infections of HFFFs at low MOI (0.01 PFU/cell) demonstrated that RCMV1111 grew with kinetics comparable to those of Merlin (p5) (Figure 3B).

In generating RCMV1111, the BAC vector was excised from the genome to leave only a residual sequence of 40 bp between US28 and US29. Intracellular FACS indicated that RCMV1111 expressed the US28 protein during the course of productive infection at an abundance comparable with Merlin (p5) (Figure 3C). Since an antibody was not available for the US29 protein, US29 transcript levels expressed by RCMV1111 and Merlin (p5) were measured by quantitative RT-PCR (QRT-PCR) (Figure 3D), using UL123 (IE1) as a standard, and were comparable. Thus, the residual 40 bp in RCMV1111 had no discernible effect on expression of the adjacent US28 and US29 genes.

Expression of eGFP by virus generated from the Merlin BAC. To facilitate the characterization of viruses generated from Merlin BACs, an IRES-eGFP expression cassette was inserted into pAL1111 immediately downstream from UL122 (IE2), so that expression was under the control of the major IE promoter (60), generating pAL1158. In the resulting virus (RCMV1158), eGFP was expressed with IE kinetics (data not shown). In growth studies performed at low MOI (0.01 PFU/cell) in HFFFs, RCMV1158 exhibited a small but consistent reduction in levels of virus production (2-fold) at 12 days post-infection (PI) (Figure 3E).

Repair of RL13 or UL128 results in growth defects in fibroblasts. In order to reconstitute the complete HCMV gene complement, the lesions in UL128 and RL13 in pAL1111 were repaired seamlessly by recombineering, both singly and in combination, culminating in a set of 4 BACs (pAL1111, pAL1119, pAL1120, and pAL1128; Table 3). The complete sequence of the fully repaired BAC (pAL1128) was verified by Solexa sequencing. A corresponding set of eGFP-tagged BACs was also constructed (pAL1158, pAL1159, pAL1160, and pAL1161; Table 3).

To assess the efficiency of virus spread from cell to cell, the 4 eGFP-tagged BACs were transfected individually into HFFFs, the cells were overlaid, and then plaque areas were measured at 3 weeks post-transfection (PT) (Figure 4 and Figure 5A). Comparable results were obtained using the BACs lacking the eGFP tag (data not shown). Viruses with either RL13 (RCMV1159) or UL128 (RCMV1160) repaired produced much smaller plaques than the double mutant (RCMV1158). Furthermore, the virus (RCMV1161) with both genes repaired produced even smaller plaques. RL13 and UL128 thus act independently to restrict either cell-to-cell transmission or virus production in fibroblast cultures.

To investigate further, HFFFs transfected with the eGFP-tagged BACs without overlay were monitored over time. Plaques formed initially by viruses with UL128, RL13, or both genes repaired (RCMV1159, RCMV1160, and RCMV1161) were subsequently outgrown by uninfected cells. To encourage virus dissemination, cells transfected with pAL1159, pAL1160, or pAL1161 were trypsinized at 7-day intervals and reseeded in the same flask without the addition or removal of cells. The eGFP reporter gene was used to identify infected cells (Figure 5B), and cell-free virus levels were measured by titration (Figure 5C). The rates of virus spread through the monolayer (Figure 5B) were consistent with the

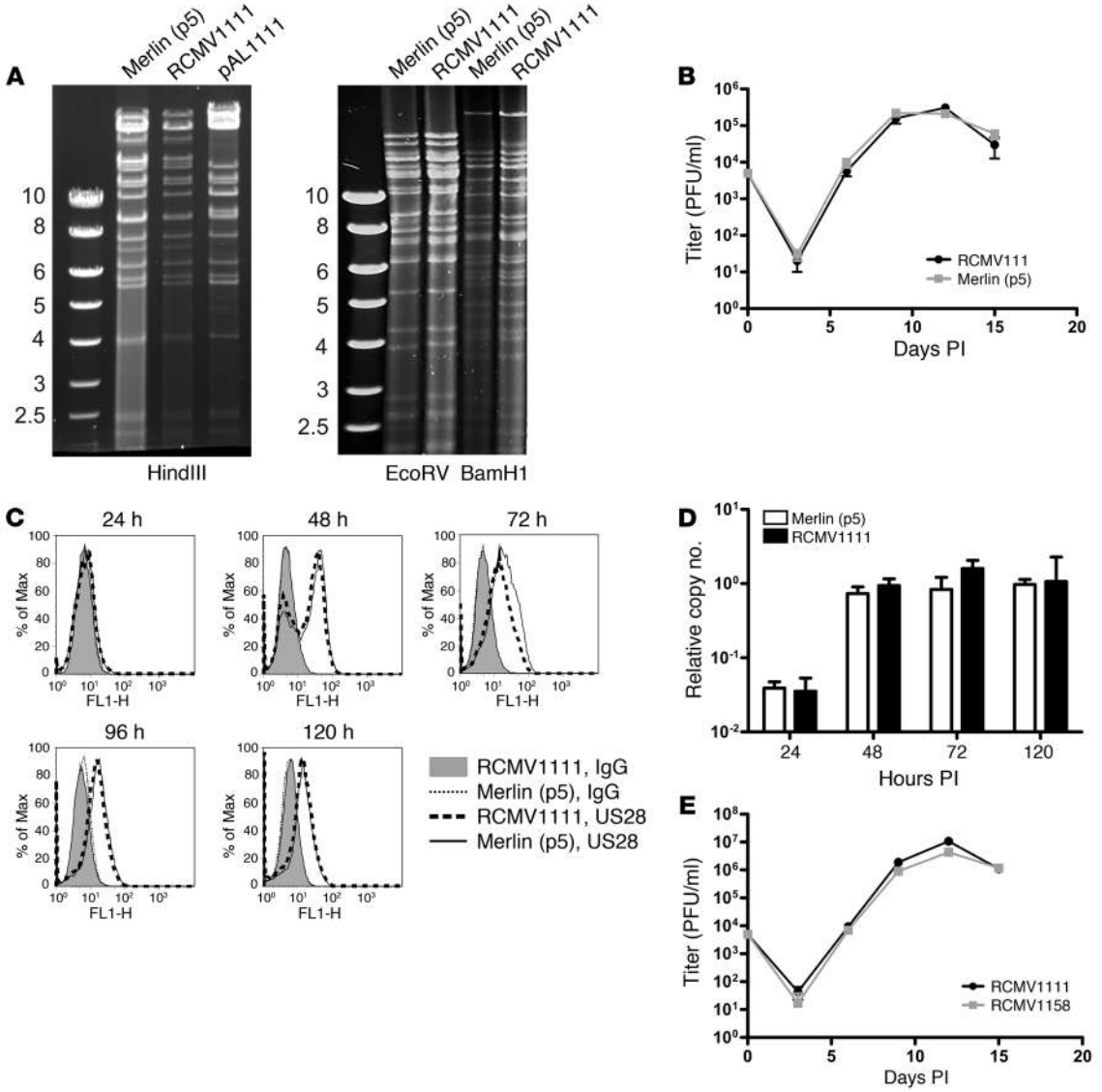

Figure 3

Properties of Merlin BAC–derived virus RCMV1111. (**A**) Restriction endonuclease profiles of DNA extracted from Merlin (p5), RCMV1111 (the virus derived from pAL1111), and pAL1111. Markers (kb) are shown. (**B**) Virus titers released into the medium following infection of HFFFs at an MOI of 0.01 PFU/cell. Error bars show mean ± SD; results are representative of 2 experiments. (**C**) Intracellular FACS staining for the US28 protein in cells at various times PI with either Merlin (p5) or RCMV1111. Controls in the form of samples stained with IgG are shown. (**D**) Copy numbers of US29 transcripts relative to UL123 (IE1) transcripts at various times PI with Merlin (p5) or RCMV1111. Figures were averaged from 3 experiments; error bars show mean ± SD. (**E**) Virus titers released into the medium following infection of HFFFs at an MOI of 0.01 PFU/ml with RCMV1158 or RCMV1111. Error bars show mean ± SD; results are representative of 2 experiments.

relative plaque sizes (Figure 5A), with slowest growth occurring when RL13 and UL128 were both repaired (Figure 5, A–C). Repairing either RL13 or UL128 also gave a clear reduction in the levels of infectious virus released into the supernatant (Figure 5C). Repairing both genes delayed dissemination of the infection through the monolayer, but substantial and increasing amounts of infectious virus were released by 5–7 weeks PT (Figure 5C).

In titrations conducted to generate Figure 5C, the plaque sizes were largely in accord with those reported in Figure 5A. However, some plaques from the repaired viruses were substantially larger than the majority. Plaque sizes were measured at the earliest time point possible: 2 weeks PT for RCMV1158, 3 weeks PT for RCMV1159 and RCMV1160, and 4 weeks PT for RCMV1161 (Figure 5D). Two clearly distinct plaque sizes were evident for RCMV1159. The 3 larger plaques were expanded individually in HFFFs, and RL13 was amplified by PCR and sequenced. Each virus contained the same 2 mutations in RL13, specifically C → A at nt 11286 (resulting in S → Y) and C → G at nt 11436 (resulting in the introduction of an in-frame stop codon). Sequencing of viruses derived from the 3 largest RCMV1161 plaques did not reveal any mutations in RL13 or UL128L.

Repairing RL13 results in growth defects in epithelial cells. Restoration of RL13 independently of UL128 suppressed virus replication in fibroblasts, with approximately 10% of virus having remutated in

Table 3
WT (+), mutated (–) status of RL13 and UL128 in Merlin BACs

BAC	Derived virus	RL13	UL128
BACs containing no tags			
pAL1111	RCMV1111	–	–
pAL1119	RCMV1119	+	–
pAL1120	RCMV1120	–	+
pAL1128	RCMV1128	+	+
BACs tagged with eGFP			
pAL1158	RCMV1158	–	–
pAL1159	RCMV1159	+	–
pAL1160	RCMV1160	–	+
pAL1161	RCMV1161	+	+
BACs containing RL13 tagged with a V5 epitope			
pAL1279	RCMV1279	+	–
pAL1280	RCMV1280	+	+
BACs tagged with eGFP, tet Operators before RL13/UL128L			
pAL1393	RCMV1393	–	+ (tet0)
pAL1448	RCMV1448	+ (tet0)	–
pAL1498	RCMV1498	+ (tet0)	+ (tet0)

RL13 by 3 weeks PT (see above; Figure 5D). To determine whether this effect was limited to fibroblasts or whether RL13 may be advantageous in other cell types (as is the case for UL128L), retinal pigmented epithelial cells (ARPE-19s) were transfected with pAL1160 or pAL1161 (Table 3) and the size of plaques was measured (Figure 6A). At all time points measured, plaques from the virus lacking RL13 (pAL1160) were larger than those from the virus in which RL13 had been repaired (pAL1161). Therefore, RL13 conferred a growth restriction in epithelial cells as well as fibroblasts. In contrast, UL128L is known to confer a restriction only in fibroblasts.

Cell cultures transfected with the eGFP-tagged BACs were monitored simultaneously for the number of infected cells (Figure 6B) and amount of infectious virus released into the supernatant (Figure 6C). The lack of growth of UL128 mutants (RCMV1158 and RCMV1159) in ARPE-19s (data not shown) was consistent with previous observations that UL128L is essential for epithelial cell tropism. As was the case with HFFFs, plaques generated by viruses in which UL128 was repaired (RCMV1160 and RCMV1161) were eventually overgrown by uninfected cells, and virus dissemination required periodic reseeding of the monolayer. Both RCMV1160 and RCMV1161 grew much more slowly in ARPE-19s than HFFFs, and, unlike HFFFs, ARPE-19s did not attain complete infection (Figure 6B), instead reaching a plateau and forming a chronic infection. The virus in which both UL128 and RL13 were repaired (RCMV1161) grew much more slowly than RCMV1160 and formed a chronic infection in which a much lower proportion of cells was infected (approximately 15% for RCMV1161 compared with 35% for RCMV1160). RCMV1161 also produced lower levels of cell-free virus than RCMV1160 (Figure 6C). This effect was only partially attributable to the lower numbers of infected cells, since RCMV1161 infected about half the number of cells as did RCMV1160 and yet produced over 10-fold less cell-free virus. Comparable results were obtained using viruses lacking the eGFP marker. Thus, repairing RL13 results in slower cell-to-cell spread and reduced levels of cell-free virus from epithelial cells as well as fibroblasts.

Rapid generation and selection of RL13 and UL128L mutants in fibroblasts. To generate working stocks of BAC-derived viruses in HFFFs, the cells in a 25-cm^2 flask were transfected with BAC DNA and reseeded periodically until 100% were infected. Cell-free virus was transferred to a single 150 cm^2 flask and then to five 150 cm^2 flasks, and virus stocks (p3) were prepared. To test the genetic integrity of the virus, 10 PCR clones each of RL13 and UL128L were sequenced. Differences from the original sequences were excluded as probable PCR errors if they were detected in single clones. An analysis of 13 virus stocks (Table 4), each derived independently from BAC DNA, found that (a) when only RL13 was repaired, it mutated in all stocks (stocks 1–4); (b) when only UL128 was repaired, the UL128 locus mutated in 2 of 3 HFFF derived stocks (stocks 5, 6), whereas it remained intact in epithelial derived stocks (stocks 8, 9; a synonymous substitution was detected in one instance); and (c) when both RL13 and UL128 were repaired, RL13 mutated in 1 stock (stock 11), whereas the UL128 locus appeared to remain intact. When the stock (stock 11) containing an RL13$^+$UL128$^+$ virus that harbored a frameshift in RL13 in 20% of genomes was passaged a fourth time, the RL13 mutation was then observed in 100% of clones, along with a deletion compromising both UL128 and UL130 in the UL128 locus. Thus, both RL13 and the UL128 locus remutated in fibroblasts, with the former tending to mutate more rapidly.

RL13 encodes a virion envelope protein. Since RL13 has not previously been characterized, it was important to establish and investigate its expression. RL13 was therefore tagged with a sequence encoding a C-terminal V5 epitope and inserted into a recombinant adenovirus (RAd) vector. The V5 epitope was also fused to RL13 within the strain Merlin BACs, in both a UL128$^-$ (RCMV1279) and a UL128$^+$ (RCMV1280) background (Table 3). The primary translation product of RL13 is predicted to be a 35-kDa protein containing a signal sequence, a transmembrane domain, 7 potential N-linked glycosylation sites, and 26 potential O-linked glycosylation sites. When RL13V5 was expressed in isolation using the RAd vector, 80-kDa and 55-kDa proteins were detected (Figure 7A), whereas 100-kDa and 55-kDa species were detected in cells infected with RCMV1279 (RL13V5$^+$UL128$^-$; Figure 7B). The 55-kDa proteins were susceptible to EndoH digestion, indicative of them being an ER-retained immature form, whereas the 80- and 100-kDa proteins were resis-

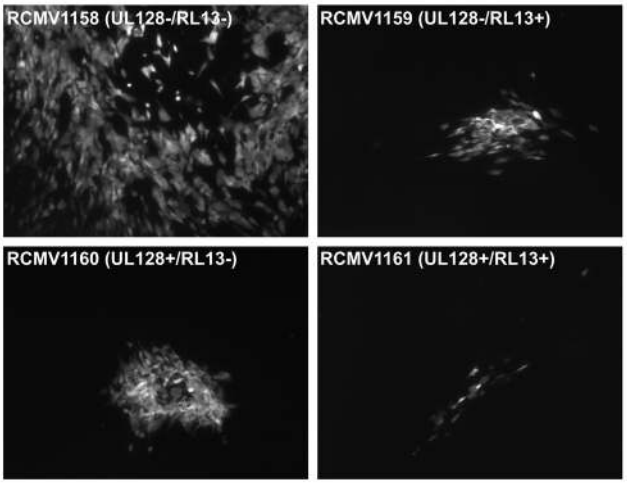

Figure 4
Growth of BAC-derived viruses in HFFFs. Images show eGFP expressed by plaques formed in HFFFs 3 weeks PT with BAC DNA as indicated. Scale bars: 100 μm.

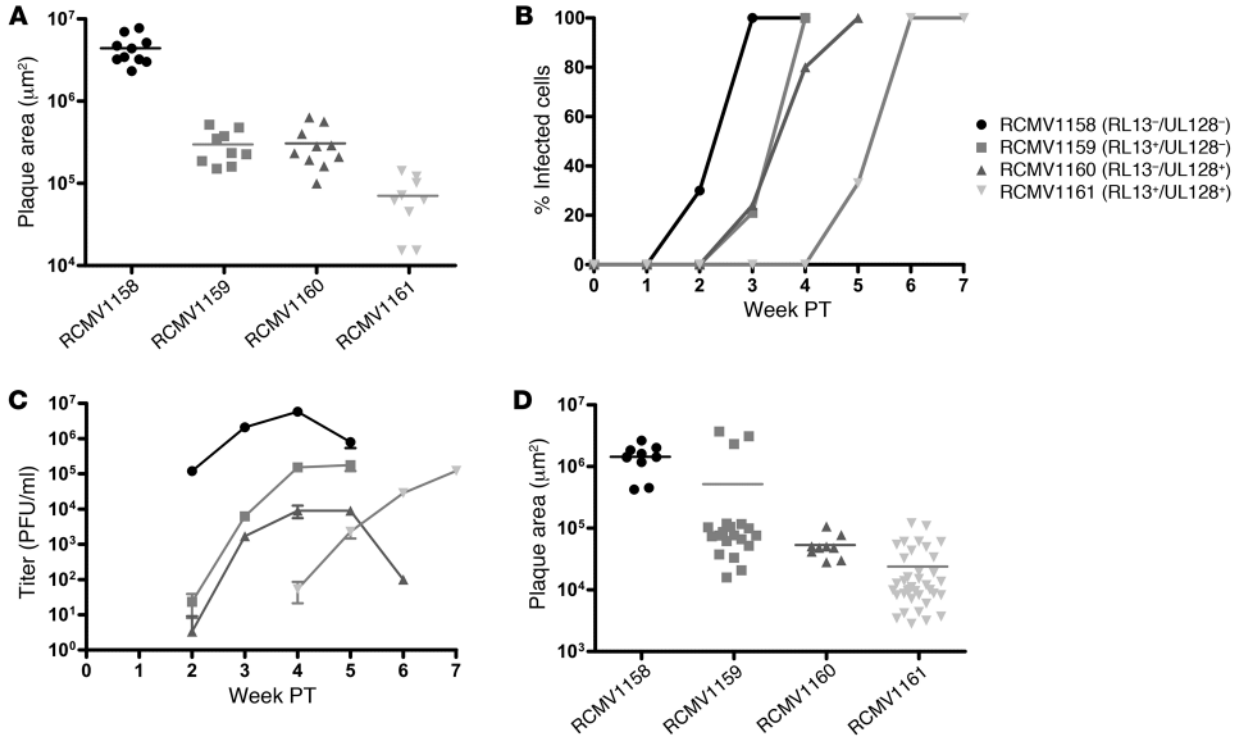

Figure 5
Growth of BAC-derived viruses in HFFFs. (**A**) Areas of individual plaques at 3 weeks PT, with cells overlaid to prevent cell-free spread of virus. (**B**) Kinetics of infection measured by FACS analysis. (**C**) Kinetics of infectious virus release into the medium of the cultures in **B**, with error bars showing mean ± SD. (**D**) Area of plaques generated by virus harvested from the media in **C**, with each sample derived from the earliest time point at which more than 10 plaques were visible.

tant to EndoH digestion and are thus presumably fully mature. PNGaseF digestion reduced the 55-kDa proteins to 35 kDa and, in addition, reduced the 80- and 100-kDa proteins to 57 and 65 kDa, respectively. Since neither enzyme was able to reduce the 80- and 100-kDa proteins to 35 kDa, it is likely that mature gpRL13 contains O-linked, as well as N-linked, sugars. Identical results were obtained with cells infected with RCMV1280 (RL13V5$^+$UL128$^+$), and no bands were seen using lysates from RL13$^-$ virus (data not shown). The observation that gpRL13 appears to be more extensively glycosylated in the context of HCMV infection than when expressed in isolation is consistent with previous observations on CD155 and gpUL18, to the effect that HCMV infection alters normal cellular glycosylation processes (22, 61).

The V5 epitope was also used to track gpRL13 expression by immunofluorescence. When RL13V5 was expressed using the RAd vector, gpRL13 trafficked to discrete cytoplasmic vesicles, a proportion of which could be stained with the early endosomal marker Rab5A (Figure 7C). This observation is consistent with much of the protein having transited the Golgi apparatus. In the context of a productive HCMV infection, the intracellular distribution of gpRL13 was different. The protein localized to the cytoplasmic site of virion assembly and colocalized in both HFFFs and ARPE-19s with a marker for the trans-Golgi network (TGN46) and pp28 (an outer tegument protein encoded by gene UL99 that interacts with the envelope and is acquired by the virion in the cytoplasm; Figure 7D) and gH (a virion envelope glycoprotein encoded by gene UL75; Figure 7E).

The finding that gpRL13 is a glycoprotein that tracks to the site of virion assembly raised the possibility that it might be a virion surface envelope protein. Growth of RL13$^+$ HCMV in vitro is inefficient, and spontaneous mutants will arise and be rapidly selected (see above). Nevertheless, we found that limited, short-term growth of RL13$^+$ virus could be fostered by sequential reseeding of cultures (Figure 5), and the antibody to a C-terminal tag would preferentially recognize full-length, nonmutated gpRL13 even if a proportion of mutants had arisen during passage. In virions purified from such cultures, only the 100-kDa mature, Endo H–resistant form of gpRL13 was detected. In virion fractionation studies, this protein copurified with glycoprotein B (gB; the product of gene UL55) in the soluble envelope fraction, rather than with pp65 (the product of gene UL83) in the tegument (Figure 8A). The V5 epitope is predicted to be located topologically on the inner side of the envelope, and this orientation was supported by immunoelectron microscopy, in which gold-labeled secondary antibody exhibited extensive labeling around the inner surface of the envelope (Figure 8B).

Conditional expression of RL13 and UL128L. The BAC pAL1111 (RL13$^-$UL128$^-$) has utility as a reproducible source of fully characterized, clonal HCMV that exhibits good genetic stability and rapid growth to high titers in fibroblasts. We also show above that short-term experiments can be performed using the Merlin BAC in which RL13 and UL128 are repaired. The major phenotypic impact these genes have on HCMV biology emphasized the need to work with WT virus. However, the rapid emergence of mutants at these loci during amplification from Merlin BAC

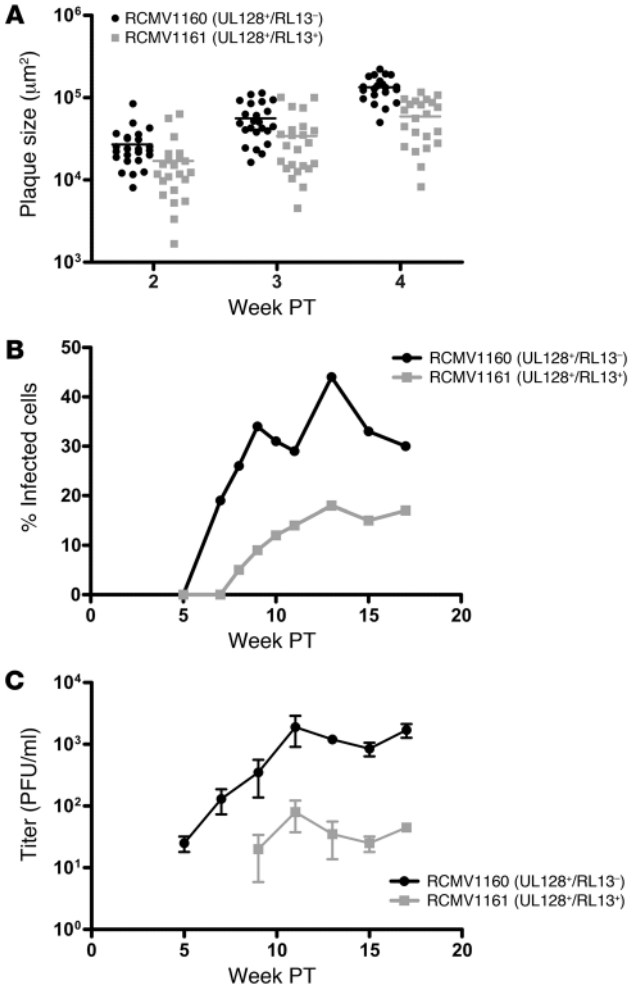

Figure 6
Growth of BAC-derived viruses in ARPE-19s. (**A**) Size of plaques at 2, 3, or 4 weeks PT, with cells overlaid to prevent cell-free spread of virus. (**B**) Kinetics of infection following transfection of BACs into ARPE-19s without overlay, measured by FACS analysis of eGFP. (**C**) Kinetics of infectious virus release into the medium of the cultures in **B**, with error bars showing mean ± SD.

transfections meant virus stocks were inevitably contaminated with mutants. In order to enable studies with phenotypically WT virus, we sought to suppress expression of RL13 and the UL128 locus during virus expansion following Merlin BAC transfection. To achieve this, hTERT-immortalized HFFFs were transduced with a retrovirus encoding the tet repressor containing a C-terminal nuclear localization signal (NLS) and tet operators were inserted upstream of the translation initiation codon of the gene to be modulated (62, 63). In HFFF-tet cells, the tet repressor binds to the tet operators and prevents transcription of the target gene, whereas transcription proceeds as normal in parental HFFFs. When tested with a RAd-expressing tet-regulated GFP, expression levels in HFFF-tet cells were reduced 180-fold relative to parental HFFFs, showing little more fluorescence than cells infected with an empty vector control (Figure 9A).

The transcriptional initiation sites for RL13 are located approximately 30- and 110-bp upstream from the translational initiation codon (K. Baluchova, unpublished observations). Transcription of UL128 starts within the UL130 coding region, and an mRNA initiating approximately 10 bp upstream of UL131A potentially encodes both the UL131A and UL130 proteins (26, 43). tet operators were inserted in various locations upstream from the RL13 or UL131A coding regions, and their capacity to selectively promote replication of RL13$^+$ or UL128$^+$ viruses in HFFF-tet cells was tested empirically. The optimal location for the tet operators was determined to be a single tet operator 19 bp upstream of RL13 (pAL1448) and 2 tet operators 33 bp upstream of UL131A (pAL1393; Table 3). Plaque formation was inhibited approximately 10-fold in HFFF cells by the presence of an intact UL128 locus, and this inhibition was relieved by infection of HFFF-tet cells with a tet-controlled UL131A virus, RCMV1393 (Figure 9, B and C). Similarly, plaque formation was inhibited approximately 10-fold in HFFF cells by the presence of an intact RL13, and this inhibition was relieved by infection of HFFF-tet cells with a tet-controlled RL13 virus, RCMV1448 (Figure 9, D and E). Titers of tet-controlled viruses obtained from HFFF-tet cells were increased 18- to 32-fold relative to the non-tet–controlled viruses (Figure 9F). In addition, sequencing of 10 PCR clones of UL128L and RL13 from RCMV1393 and RCMV1448, respectively, showed all contained the WT sequence. Following passage in HFFFs with this RCMV1393 stock, virus was able to infect ARPE19 cells and produced plaques of a size equivalent to the non–tet-controlled parental virus RCMV1160 (Figure 9G). Finally, having verified that both RL13 and UL131A could be independently tet-controlled, a virus was constructed in which both genes contained tet operators upstream of their ATG codons. Like the previous constructs, plaque formation was inhibited in HFFF cells by the presence of an intact RL13 and UL128 locus, and this repression was relieved by infection of HFFF-tet cells with a virus in which both RL13 and UL128 were tet-controlled (RCMV1498) (Figure 10, A and B).

Thus, repression of RL13 and UL131A in HFFF-tet cells demonstrably provides a means to amplify Merlin virions containing intact versions of RL13 and the UL128 locus. Two options are available to produce phenotypically WT HCMV from these viruses: either transcriptional repression can be released by the addition of doxycycline to infected HFFF-tet cells or, as demonstrated above, a final replication cycle can be performed in HFFFs.

Discussion

Diagnostic laboratories have long recognized that HCMV strains in clinical samples do not adapt readily to cell culture. Our construction of what we believe is the first BAC containing a complete, characterized copy of a genetically intact HCMV genome provides an explanation for this phenomenon in showing that adaptation is dependent on 2 independent mutations, one in the UL128 locus (previously recognized; ref. 26) and one in RL13 (identified in the present study). To date, HCMV research has by necessity used viruses that, to varying degrees, are compromised genetically. Although laboratory-adapted viruses have proved invaluable, there is a clear need to develop systems that represent the WT virus responsible for clinical disease. To this end, the Merlin genome (p5) was cloned using BAC technology, and the sequence of an initial BAC (pAL1053) was compared with that of the parental strain. Specific issues relating to tissue culture adaptation were clarified and resolved using sequence data derived directly from the original clin-

Table 4
RL13 and UL128L mutations detected by PCR in BAC-derived viruses at p3

Stock	RL13 mutations				UL128L mutations			
	Mutation	Position	Affected clones (%)	Effect	Mutation	Position	Affected clones (%)	Effect
RL13$^+$UL128$^-$ BAC transfected into HFFFs								
1	^A	11363	33	*f*				
1	G → T	11901	40	E → X				
2	ΔA	11363	30	*f*				
3	^A	11363	50	*f*				
4	A → G	11297	20	S → G				
4	C → T	11427	20	A → V				
4	A → G	11956	20	I → M				
RL13$^-$UL128$^+$ BAC transfected into HFFFs								
5					C → T	176229	14	R → Q
5					T → C	176845	14	I → V
5					CAAGA → TCTTG	176915-9	21	FL → SA
6					ΔT	176456	30	None (intron)
7					None		100	None
RL13$^-$UL128$^+$ BAC transfected into ARPE-19s								
8					None		100	None
9					A → G	176917	20	None
RL13$^+$UL128$^+$ transfected into HFFFs								
10	None		100		ΔT	176456	50	None (intron)
11	^A	11363	20	*f*	None		100	None
12	None		100		ΔT	176456	30	None (intron)
13	None		100		ΔT	176456	30	None (intron)

Each row represents an individual virus stock. Nt positions are given with respect to NC_006273. +, WT gene; –, mutated gene; ^, inserted nt; Δ, deleted nt.

ical sample that gave rise to Merlin. Mutations that affected HCMV coding regions were sequentially repaired by recombineering, so that the only relic in virus recovered from BACs by DNA transfection was a 40-bp sequence containing a *loxP* and an NheI site located between the US28 and US29 coding regions. The presence of this sequence did not affect expression of the flanking genes.

The high level of sequence identity between pAL1053 and strain Merlin (p3) demonstrated that the HCMV genome had suffered minimal perturbation during BAC cloning. In pAL1053, nonsynonymous mutations in protein-coding regions were identified in UL36, UL128, and RL13. The differences in UL36 were specific to pAL1053 and its predecessor, pAL1031, and were presumably derived from a small proportion of mutants that arose in cell culture. HCMV and rhesus cytomegalovirus strains have previously been found to have acquired inactivating mutations in UL36 following passage in vitro, implying that there may be some selective pressure for such mutants (14, 64). Following repair of UL36, the resulting BAC (pAL1111) provided a reproducible source of clonal HCMV strain Merlin (RCMV1111; RL13$^-$UL128$^-$; Table 3), whose growth properties were indistinguishable from the parental virus. BACs in which either RL13, UL128, or both genes were repaired were generated from pAL1111 and supplemented by a corresponding series of BACs containing an eGFP marker. pAL1128 and pAL1161 contain the complete HCMV gene complement and, for what we believe is the first time, enabled experiments to be undertaken with a clonal population of effectively WT virus. Although RCMV1111 and its eGFP-expressing counterpart (RCMV1158) were stable during limited culture and suitable for generation of high-titer virus stocks, repair of UL128 or RL13 (or both) severely impaired HCMV growth in HFFFs, and propagation of these viruses was associated with rapid selection of further mutants at these loci. Therefore, we developed the HFFF-tet cell line, which allowed RL13 or UL131A to be repressed during recovery of virus from the BAC, thus providing a stable platform for experimentation on genetically intact HCMV.

Although HCMV replication has been described in a wide range of cell types, efficient virus production in vitro has been achieved only using viruses adapted to growth in fibroblasts. Indeed, existing cell-culture systems appear to be essentially incompatible with efficient propagation of WT HCMV. HCMV is not exceptional in this regard. Of the 8 known human herpesviruses, only WT herpes simplex virus types 1 and 2 (HSV-1 and HSV-2) can be propagated readily to high titer in cell culture. Nonetheless, very high HCMV virus loads are often detected in urine samples from congenitally infected neonates (as was the case for the sample from which Merlin was isolated), and this indicates that conditions exist in vivo that are compatible with efficient replication of WT HCMV. It is possible that RL13 regulates a switch to productive HCMV replication in vivo.

The UL128 locus is essential for the efficient infection of epithelial and endothelial cells by HCMV (37–43) but is detrimental to growth in fibroblasts. Consequently, mutants in this locus are selected when clinical isolates are passaged in fibroblasts (12, 26, 27, 44, 45, 47, 48). Merlin was originally selected for detailed investigation from a series of clinical isolates partly on the basis of its excellent growth properties in fibroblasts. However, this process favored the selection of a UL128 mutant, which emerged during p1 (26). When the lesion was repaired in the BACs, alternative defects in the UL128 locus emerged by p3–p4. In other studies monitoring endothelial cell tropism in clinical isolates, loss of phenotype has been reported in fibroblasts after p20 (44), p22 (45), or p15–p20 (28). Such studies defined a virus "passage" as corresponding to

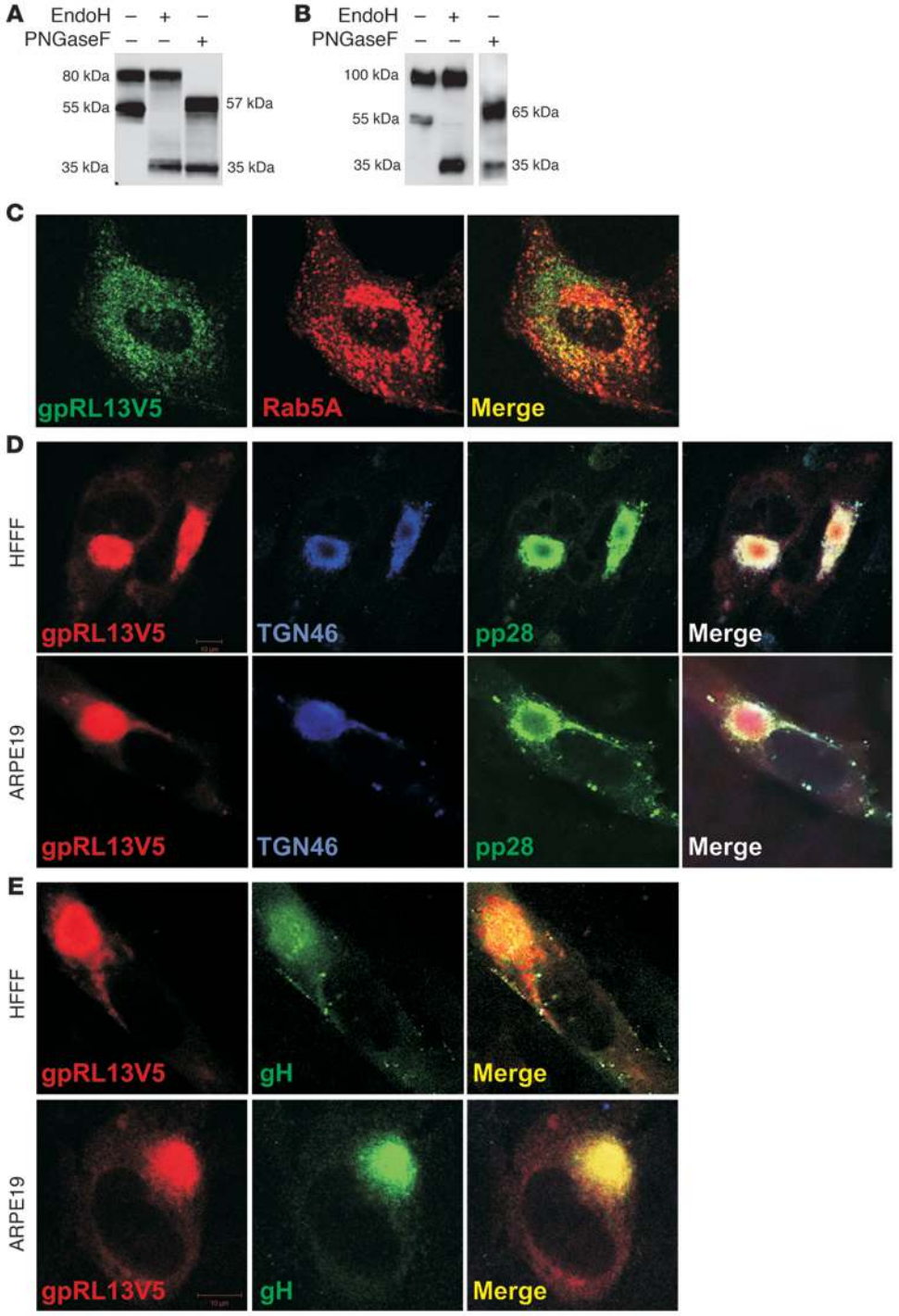

Figure 7
Characterization of gpRL13. (**A** and **B**) Western blot performed on RL13V5, showing the sizes of the proteins in native form or following digestion with EndoH or PNGaseF. RL13V5 was either expressed in isolation from a RAd (**A**) or from its native position in RCMV1279 (**B**). (**C**) Immunofluorescence performed for the indicated antigens on HFFFs infected with the RAd expressing RL13V5 (×640 magnification). (**D** and **E**) Immunofluorescence performed for the indicated antigens either on HFFFs infected with RCMV1279 or on ARPE-19s infected with RCMV1280. Original magnification, ×640.

each serial subculture (usually weekly) of an infected cell monolayer. However, in the present study, virus passage involved destruction of the entire cell monolayer following infection with cell-free virus, a process that normally involves many more cycles of virus replication. Also, given that viruses mutated in the UL128 locus released higher amounts of virus into the medium, our use of cell-free virus may have further encouraged the selection of mutants.

The identification of an RL13 mutation in pAL1053 was unexpected because the genome sequence of Merlin (p3) indicated that this coding region was intact (27). It led to the discovery that low-passage Merlin stocks actually consisted of mixtures of various different RL13 mutants. This finding brings a resolution with observations that almost all HCMV strains and BACs are overtly mutated in RL13 (27). Parallels exist between RL13 and the UL128 locus in the fact that mutations arise in both genes during adaptation to culture in fibroblasts. However, it is clear that RL13 and the UL128 locus can function independently because either gene in intact form was capable of suppressing virus replication, and

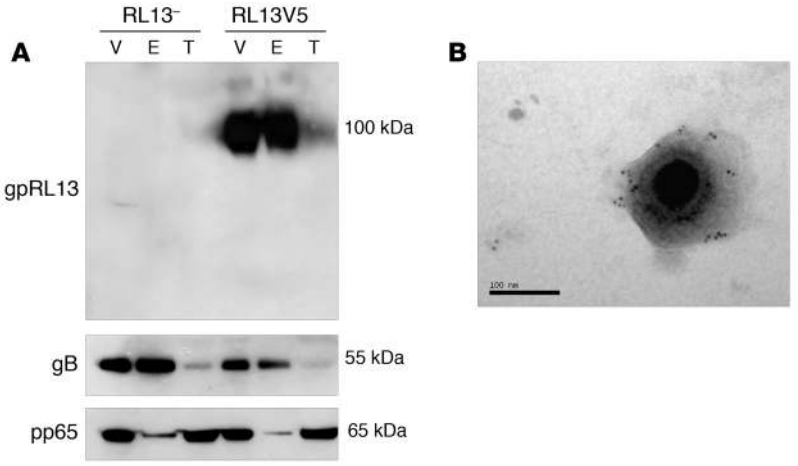

Figure 8
Localization of RL13 in the virion. (**A**) Western blot performed on purified virions from virus expressing a truncated gpRL13 (RCMV1111, RL13–) or full-length RL13 with a C-terminal epitope tag, gpRL13V5 (RCMV1279, RL13+). Complete virions (V), envelope fraction (E), and tegument/capsid fraction (T) were probed for the antigens indicated. (**B**) Immunogold EM staining for RL13V5 in purified RCMV1279 virions. Original magnification, ×40,000.

repair of both had an additive effect. The RL13 phenotype was also shown to be distinct from that of the UL128 locus, since RL13 suppressed HCMV replication in both fibroblasts and epithelial cells, whereas the UL128 locus was not only stable, but promoted infection, in epithelial cells. Nevertheless, the finding that gpRL13 is present in the virion indicates that it may have a role in modifying tropism (similar to the UL128 locus) or in modulating cell signaling during virus entry (as proposed for gB).

The apparent ease with which RL13 mutants were selected in cell culture raised the possibility that they preexisted in the clinical sample, perhaps reflecting the potential for an expanded cell tropism in vivo. This possibility is technically challenging to disprove, since such mutants might be present in very low proportions. However, we were unable to detect the existence of RL13 mutants in the primary clinical sample from which Merlin was derived. It was estimated that approximately 10^6 particles were used in the initial infection of a 25-cm^2 flask to isolate Merlin, and this would have resulted in most cells receiving a particle. Nonetheless, passage 1 of Merlin took 4 weeks to complete. The mutation rate of DNA viruses is relatively low and has been calculated at 0.003 per genome replication for HSV-1 (65). If this value holds for HCMV, mutants in the UL128 locus and/or RL13 would be expected to arise during p1. This mutation rate operating on 10^6 viruses would result in a total of 3,000 mutations per genome replication. Since RL13 accounts for 879/235,646 bp in strain Merlin genome, approximately 11 mutations would be in RL13. The acquisition of mutations in both RL13 and UL128 could have resulted either from sequential mutations in the same template or as a result of recombination between independent mutants. Despite the counterintuitive nature of such rapid selection events in a herpesvirus, mutations in RL13 and the UL128 locus were also identified at p3 following transfection of the repaired BACs into HFFFs, and these were clearly generated de novo. Interestingly, mutants emerged in RL13 more rapidly than in the UL128 locus. Some data also indicated that RL13 may mutate more rapidly in the context of UL128 mutated viruses; however, this may simply reflect the slower growth of the WT virus.

In support of our conclusions concerning the instability of RL13 in cell culture, a collaborative study has shown that RL13 mutants were invariably selected in fibroblasts, epithelial, and endothelial cells during sequential passage of HCMV strains from clinical samples (28). Also, in most existing HCMV BACs (including FIX, Ph, Towne, Toledo, and AD169), RL13 is mutated overtly by deletions, frameshifts, or substitutions that introduce premature termination codons (27), and that derived from strain TB40/E (54) contains a unique substitution that greatly reduces the prediction of a signal peptide for gpRL13 (A.J. Davison, unpublished observations). Relating to this, we note that on 2 occasions, viruses derived from Merlin BACs replicated relatively efficiently in fibroblasts and yet retained an intact RL13 (RCMV1159 [data not shown] and a proportion of RCMV1161; see Figure 5D). This suggests that another HCMV gene may be required for RL13 function and that this gene is less prone to mutation than RL13.

HCMV exhibits the highest degree of intrastrain sequence variation of any human herpesvirus, and RL13 is a member of a small group of genes that exhibit the greatest variation (27). Also among this group are genes UL146 (27, 35, 36, 66–68) and UL74 (gO) (27, 35, 69–71), which are well characterized because of their utility in genotyping clinical isolates. The selection pressures responsible for generating such degrees of divergence are not fully understood, but their origins, and perhaps the era in which they have operated, appears to be ancient (66). Despite remarkable sequence variation among HCMV strains, UL146 and UL74 are stable within individual patients, and identical UL146 sequences have been detected in geographically distant individuals (35, 66). RL13 is one of 14 members of the RL11 gene family, which is believed to have arisen through gene duplication and then diverged during the evolution of the primate cytomegaloviruses (72). Several other members of this family are also hypervariable. As a virion envelope protein, gpRL13 may be a prime target for neutralizing antibody, and it is possible that selection is exerted on it in vivo to drive escape from the humoral immune response. In support of this, when $CD4^+$ T cell responses to HCMV were measured, RL13 was one of the top 5 most immunogenic HCMV ORFs (73). It would be interesting to determine whether RL13 is now stable or whether the mechanism driving its genetic variation remains operational.

The question arises of why RL13 is detrimental to virus replication in both epithelial and fibroblast cells in culture. The virion components encoded by the UL128 locus are clearly also detrimental in fibroblasts, yet they are essential for infection of other cell types. Since gpRL13 is also present in the virion, it may likewise modify tropism in some way that has not yet been recapitulated in vitro. Recent studies have suggested that HCMV is capable in vivo of establishing persistent, low-level infections that are cor-

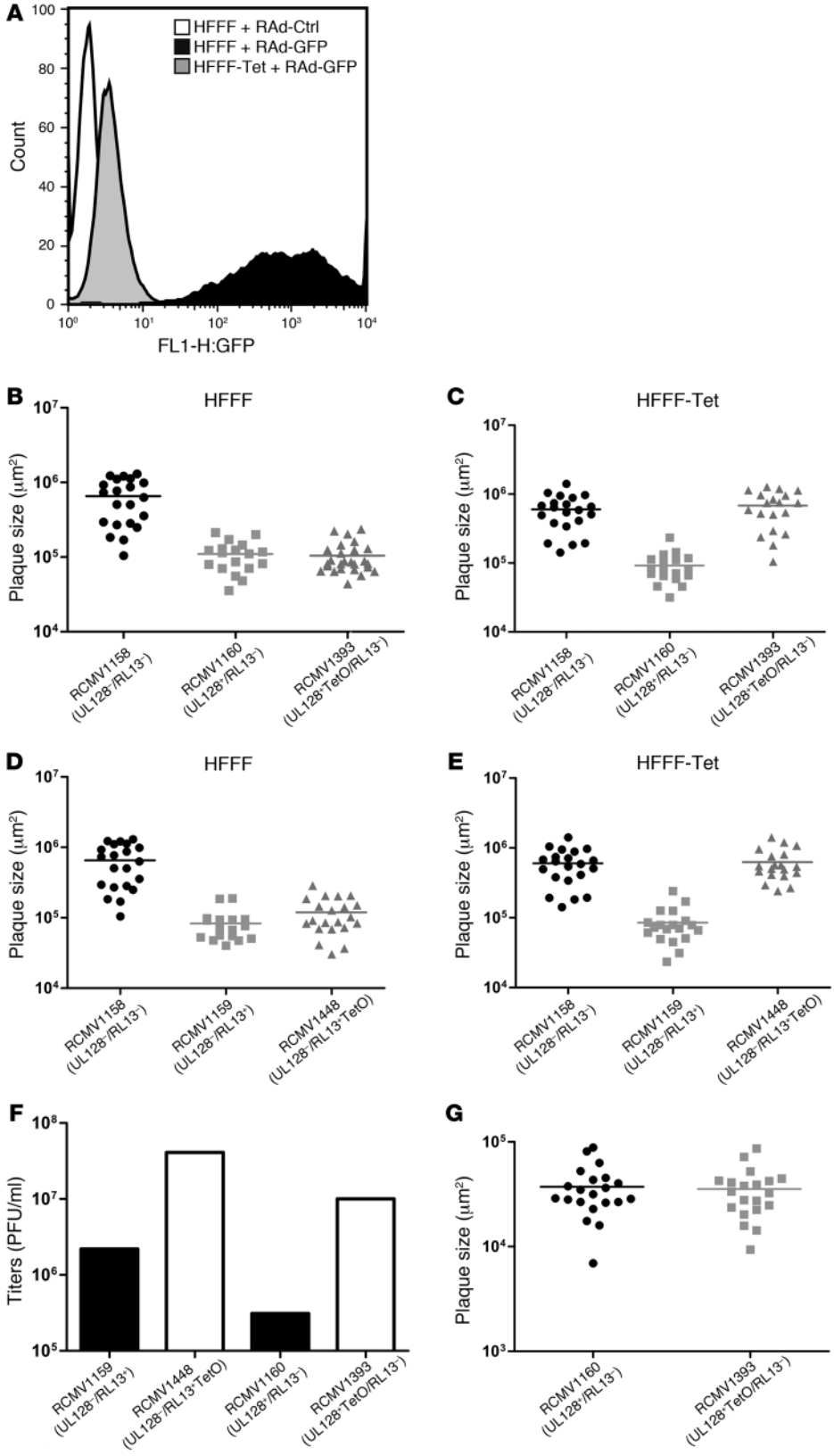

Figure 9
Repression of UL128L and RL13 by BAC-derived viruses in HFFF-tet cells. (**A**) FACS analysis of parental HFFFs or HFFF-tet cells, infected with empty control adenovirus (RAd-Ctrl) or RAd-expressing eGFP (RAd-GFP). RAd-GFP expresses GFP from the HCMV MIE promoter, containing 2 tet operators 10 bp downstream of the TATA box. (**B**–**E**) Plaque sizes of viruses generated at 2 weeks PT in HFFFs (**B** and **D**) or HFFF-tet cells (**C** and **E**), with cells overlaid to prevent cell-free spread of virus, showing (**B** and **C**) repression of UL128L in RCMV1393 and (**D** and **E**) repression of RL13 in RCMV1448. (**F**) Titers of virus stocks obtained from HFFF-tet cells infected with viruses in which RL13 and UL131A were tet controlled (RCMV1448 and RCMV1393, respectively) or the parental viruses in which RL13 and UL131A were not tet controlled (RCMV1159 and RCMV1160, respectively). (**G**) Plaque size of parental virus (RCMV1160) or virus in which UL131A was tet controlled (RCMV1393) in ARPE19 cells, 3 weeks PT.

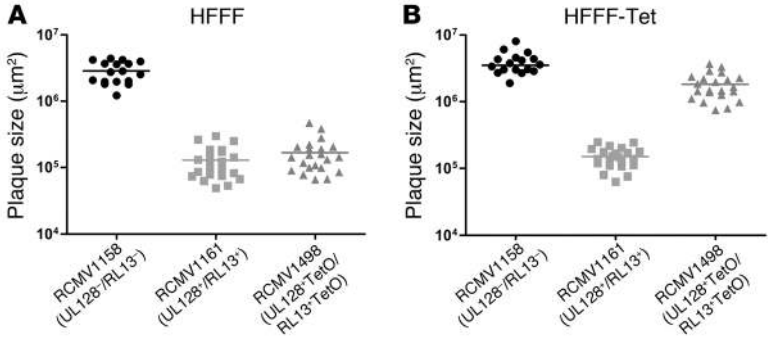

Figure 10
Simultaneous repression of UL128L and UL13 by BAC-derived viruses in HFFF-tet cells. Plaque sizes of viruses generated at 3 weeks PT in HFFFs (**A**) or HFFF-tet (**B**) cells, with cells overlaid to prevent cell-free spread of virus. Data points represent individual plaque sizes recorded for each mutant.

related with the presence of glioblastomas (74–76). Alternatively, therefore, RL13 may act as a regulator, promoting persistence of HCMV by suppressing the switch to full lytic infection until virus dissemination is required. Clearly there are situations in vivo, as illustrated by UL138 (which promotes latency by suppressing lytic infection in $CD34^+$ myeloid progenitors), where it can be beneficial for the virus to restrict or limit productive infection.

Consideration has been given to using live HCMV as a vaccination agent, vaccine carrier, and vector for gene therapy. Such studies are being developed with strains adapted to cell culture that have lost RL13 function. When the low passage HCMV strain Toledo was evaluated in human virus challenge, mild to severe disease was induced in immunocompetent individuals (both seronegative and seropositive) receiving doses ranging between 10 and 1,000 PFU (9). Indeed, the capacity of this strain to induce clinical disease was impressive. However, Toledo is known to have a large, in-frame deletion in RL13 and an ablation of UL128 (27). The absence of RL13 function as a repressor of HCMV replication could potentially have enhanced the efficiency of Toledo replication, dissemination, and pathogenesis during an acute infection. In addition to demonstrating that RL13 is incompatible with efficient virus replication in vitro, we have now provided a method for conditional expression of RL13 and UL131A in the context of productive virus infection in HFFFs. The system that we have developed will facilitate HCMV studies with virus fully representing the clinical agent.

Methods

All studies in human and animal cells were approved by Bro Taf Local Research Ethics Committee, Cardiff, United Kingdom.

Cells and viruses. HFFFs and ARPE-19s (77) were grown in DMEM (Gibco; Invitrogen) containing 10% FCS (Gibco; Invitrogen) at 37°C in 5% CO_2. HCMV strain Merlin (p5) (27) was utilized to generate BACs as described below. Infections were performed as described previously (78), and viruses were titrated in triplicate by plaque assay for 14 days on HFFFs using a 1% Avicel overlay (79). Cultures that exhibited small plaques at 14 days PT were incubated for a further 14 days and recounted. Plaques were visualized using an ORCA-ER camera mounted on a Leica DMIRBE microscope, and sizes were computed using Openlab 3 software (Improvision).

PCR. Three DNA polymerases were used in PCR reactions according to the manufacturers' protocols: Phusion (NEB) for fragments greater than 4 kb; Advantage 2 (Clontech) for amplification directly from virus stocks or cultures; and Expand Hi-Fi (Roche) for all other experiments. Oligonucleotide primers were purchased from Sigma-Aldrich at desalted purity. RL13 and the UL128 locus were amplified for sequencing using primers RL13F (ATCCTGAACATGAAGACTGACGTT) and RL13R (GAATAAACACACCCAAACATTAATGAC), and UL128F (CAGAAACTCACATCGGCGACA) and UL131AR (CCATCACCTCGCCTATACTATGTG), respectively.

Isolation, transformation, and transfection of DNA. Minipreps of plasmids or BACs were produced as described previously (62). Maxipreps were produced using NucleoBond BAC100 kits (Machery Nagel) from 500 ml overnight bacterial cultures. BAC DNA transfections (2 μg) of HFFFs (10^6 cells) were performed using a basic fibroblast kit and a Nucleofector (Amaxa) according to the manufacturer's protocol. Transfections into ARPE-19s were performed in 25-cm^2 flasks using effectene (QIAGEN) according to the manufacturer's protocol for 60-mm dishes.

Transformation of *E. coli* was performed by electroporation at 2.5 kV using 2-mm cuvettes and a Micropulser (Bio-Rad). When PCR products were cloned for sequencing, DNA was purified from agarose gels using a GFX PCR DNA and Gel Band Purification kit (GE Healthcare) and cloned into pCR4-TOPO (Invitrogen) according to the manufacturer's instructions.

Construction of the BAC-targeting vector. The BAC-targeting vector (pAL1026; Figure 1) used to capture the Merlin genome contained markers for eGFP and puromycin resistance (eGFP/Puro) and homology arms matching HCMV genes US28 and US34A (817 and 888 bp, respectively), a chloramphenicol resistance gene (*cat*), genes *sopA*, *sopB*, and *sopC*, which ensure active partitioning during cell division, and gene *repE*, which mediates assembly of the replication complex in *E. coli* at Ori2. Each homology arm was flanked by a *loxP* site, and a unique NheI restriction site was positioned between them.

To generate pAL1026, pBeloBAC11 (New England Biolabs; GenBank U51113; ref. 80) was digested with HpaI and ApaLI, blunt-ended with Klenow DNA polymerase, and religated to remove the existing *cos* and *loxP* sites, thus generating pAL767. Homology arms matching genes US28 and US34 were amplified from Merlin DNA using primers US28F (GGCCGCTAGCTGGCGACGTCGGATTCAATG; NheI site underlined), US28R (GGCCGGATCC**ATAACTTCGTATAATGTATGCTATACGAAGTTAT**AGCGCTTTTTTATTACGGTATAAT; BamHI site underlined, *loxP* site shown in bold), and US34F (GGCCGCATGC**ATAACTTCGTATAGCATACATTATACGAAGTTAT**GACCAGTGGTGGCGGGGAAT; SphI site underlined, *loxP* site shown in bold) and US34R (GGCCGCTAGCGGGACTTTCATCCTGCATTA; NheI site underlined), respectively. The 2 PCR products were digested with NheI, ligated together, digested with SphI and BamHI, and inserted into pAL767, thus generating pAL799. A linker containing a PacI site was inserted into the BamHI site, and then an expression cassette encoding eGFP/Puro (under the control of an SV40 promoter and linked by an internal ribosome entry site [IRES]) was inserted into pAL799, thus generating pAL815. The eGFP/Puro expression cassette was derived from the BAC-targeting vector YD-C19 (a gift from D. Yu; ref. 53) by amplification using primers eGFP-PuroF (GGCCTTAATTAACAATTCGGCGCAGCACCA; PacI site underlined) and eGFP-PuroR (GGCCTTAATTAAGATCCAGACATGATAAGATACATTGATG; PacI site

underlined). The amplified fragment was digested with PacI and inserted into PacI-digested pAL815, thus generating pAL1026.

Construction of a Merlin BAC. 1 μg pAL1026 was linearized by NheI digestion and transfected using Effectene (QIAGEN) into 5 × 10^5 HFFFs. Cells were infected at 24 hours PT with Merlin (p5) at an MOI of 10, and recombinants were enriched by selection with puromycin (2.5 μg/ml) and detected by visualizing eGFP. When a significant proportion of cells exhibited eGFP expression, circular DNA was extracted using Hirt extraction (53, 81) and transfected into *E. coli*. Selection with chloramphenicol allowed the identification of BAC colonies, from among which pAL1031 (Figure 1) was analyzed in detail and repaired by recombineering.

Repairing of Merlin BACs. Recombineering was performed in *E. coli* SW102 using *lac*Z/*amp*^{r}/*sac*B (62) and *gal*K selection cassettes (82) as previously described. The sequences of the primers used are listed in Supplemental Table 1 (supplemental material available online with this article; doi:10.1172/JCI42955DS1). All constructs were verified by sequencing modified regions and by restriction digest at each step. To enable the Merlin UL29–UL34 sequence to be reintroduced into pAL1031, the *lac*Z/*amp*^{r}/*sac*B cassette was amplified and inserted between the *loxP* site and US34A using primers SacBF-LoxPHom and SacBR-US34AHom to generate pAL1033 (Figure 1). To generate the insert, 2 PCR products were produced, digested with NheI, and ligated together. A 482-bp region encompassing the *loxP* site adjacent to US34 in pAL1026 was amplified using primers LoxP-R (GGCCGCTAGCATAACTTCGTATAATGTATGCTATACGAAGTTATGCATGCAAGCTTGAGTATTC; NheI site underlined) and Chlor-F (GGCCAGATCTGTCGGCAGAATGCTTAATGAA; BglII site underlined). A 5.2-kb region of the Merlin genome spanning genes US29 to US34A was also amplified using primers US29F (GGCCGCTAGCACCTCGGCCTTTTCATACAA; NheI site underlined) and US34AR (GGCCAGATCTGGGACTTTCATCCTGCATTA; BglII site underlined). Each amplicon was cloned into pCR2.1-TOPO (Invitrogen) for sequencing. A clone of each amplicon in which the sequence was correct was digested with BglII/NheI. The fragments were ligated together and recombineered into pAL1033, thus replacing the *lac*Z/*amp*^{r}/*sac*B cassette by US29–US34A and generating pAL1040 (Figure 1).

The eGFP/Puro cassette in pAL1040 was replaced by a Cre recombinase gene under the control of an SV40 promoter and containing a synthetic intron (57) so that the protein would be expressed in mammalian cells but not *E. coli*. The *lac*Z/*amp*^{r}/*sac*B cassette was amplified using primers SacBF-GFPPuroHom and SacBR-GFPPuroHom and inserted into pAL1040, thus generating pAL1047 (Figure 1). The Cre recombinase expression cassette was amplified from YD-C66 (a gift from D. Yu; ref. 53), using primers CreF-SV40Hom and CreR-BACHom, and recombineered in place of the *lac*Z/*amp*^{r}/*sac*B cassette, thus generating pAL1053 (Figure 1).

The sequence of pAL1053 was determined (see below) and indicated the presence of several differences from that of WT Merlin (see Results). Redundant sequences containing residual *lac*Z sequences were deleted by replacement with a *gal*K selectable marker, which was amplified using primers GalKF-CreHom and GalKR-SopCHom. The *gal*K marker was then removed using the primer RemoveGalKBAC, thus generating pAL1090 (Figure 1). To repair the lesions in gene UL36, the *lac*Z/*amp*^{r}/*sac*B cassette was amplified using primers SacBF-UL36Hom and SacBR-UL36Hom and inserted in place of UL36. UL36 was then amplified from Merlin DNA using primers UL36F and UL36R and recombineered in place of the *lac*Z/*amp*^{r}/*sac*B cassette, thus generating pAL1111 (Figure 1). Additional BACs were generated by repairing either and then both of the UL128 and RL13 mutations by the same technique. In each case, the *lac*Z/*amp*^{r}/*sac*B cassette was amplified using primers flanking the mutation (SacBF-UL128Hom and SacBR-UL128Hom or SacBF-RL13Hom and SacBR-RL13Hom) and recombineered into the relevant BAC, and the selectable marker was excised and the mutation repaired by recombination with oligonucleotide UL128Rep or RL13Rep.

To insert an IRES-eGFP expression cassette immediately downstream from gene UL122 (IE2) into each of the 4 BACs described above, the *lac*Z/*amp*^{r}/*sac*B cassette was amplified using primers SacBF-IE2Hom and SacBR-IE2Hom. In the resulting BACs, the *lac*Z/*amp*^{r}/*sac*B cassette was replaced by an IRES-eGFP cassette amplified from pIRES2-GFP (Clontech) using primers IRESF-IE2Hom and GFPR-IE2Hom.

DNA sequencing. All PCR products in directly cloned or recombineered form were verified by sequencing using a BigDye 3.1 kit (ABI) and standard techniques, except that the number of cycles during sequencing was increased from 25 to 100. Reactions were purified using Dye Terminator Removal Columns (EdgeBio) and analyzed on an ABI Prism 3130xl Genetic Analyzer (Applied Biosystems).

Two BACs were sequenced using published approaches (59). The complete HCMV component of pAL1053 was determined via standard Staden sequencing of a set of overlapping PCR products, and that of pAL1128 in its entirety was determined using data from an Illumina Genome Analyzer (The GenePool, University of Edinburgh). The sequence of pAL1128 was deposited in GenBank as accession GU179001. All nts in the text are specified relative to Merlin (NC_006273).

QRT-PCR. QRT-PCR was performed to analyze the expression levels of gene US29 in infected cells. The cells were trypsinized and washed once in PBS, and whole-cell RNA was extracted using an RNEasy Mini Kit (QIAGEN) and DNAse-treated using Turbo DNA-free (Ambion). US29 transcripts were amplified using primers US29F (GACATCGGTGACACAGCTTCA) and US29R (CTTGGCCTTCAGAGACCGC), and UL123 (IE1) transcripts were amplified using primers IE1F (AGGAAGAAAGTGAACAGAGTGATGA) and IE1R (TTCCTCAGCACCATCCTCCT). For RT-PCR with real-time detection, an iScript One-Step RT-PCR kit with SYBR Green (Bio-Rad) was employed according to manufacturer's instructions, and samples were analyzed on an iCycler (Bio-Rad). Serial dilutions of a Merlin BAC (pAL1053; see below) were used to establish a calibration curve. Since transcripts antisense to US29 have been reported (83), the sense transcript was amplified specifically using the reverse primers (100 pmol) with 100 ng RNA in a reverse transcription step at 50°C for 10 minutes, followed by inactivating reverse transcriptase at 95°C for 5 minutes. The forward primer was then added, and the samples were cycled 40 times through 95°C for 10 seconds, 60°C 30 seconds, and 83°C for 10 seconds, with data being collected following the final step of each cycle. Melt curve analysis was performed following the 40 cycles, and amplification of a product of the correct size was confirmed by agarose gel electrophoresis. Samples were analyzed in triplicate, and the results were averaged. Samples from uninfected cells and infected cells processed without conducting the reverse transcriptase step were uniformly negative.

Flow cytometry. A Cytofix/Cytoperm plus kit (BD) was used for intracellular staining of the US28 protein, and the Tub-45 antibody (a gift from U. Höpken; ref. 84) was used (1:5) in combination with goat anti-mouse Alexa Fluor 488 (1:200) for detection (Invitrogen). HCMV infection was monitored directly by eGFP expression or indirectly by downregulation of MHC class I from the cell surface using antibody W6/32 (1:100) followed by goat anti-mouse Alexa Fluor 647 (1:200) (Invitrogen). Samples were measured on a FACSCalibur (BD), and data were analyzed in FlowJo (Treestar).

Generation of the HFFF-tet cell line. The coding region of the tet repressor was amplified using primers tetR-F (GGCCGGATCCCTATAGGGCGAATTGAT**ATG**TCTA; BamHI site underlined, initiation codon in bold) and tetR-R (GGCCGAATTC**TTATACCTTTCTCTTCTTTTTTGGATCA**GACCCACTTTCACATTTAAGTTG; EcoRI site underlined, NLS shown in bold) and cloned into the BamHI/EcoRI sites of the retrovirus vector pMXs-IP (85). Retrovirus stocks were produced by transfecting 293Phoenix

packaging cells (86) using Effectene (QIAGEN) according to manufacturer's instructions and harvesting the supernatant 48 hours PT. Retrovirus was bound to culture dishes with Retronectin (Clontech) and used to infect hTERT-immortalized HFFFs. The cells were selected in puromycin (1 μg/ml) at 48 hours PI.

Inserting tet operators into BACs. tet operators were inserted by recombineering. To insert 1 tet operator 19 bp upstream of the RL13 coding region, the *lacZ*/*amp*^{r}/*sac*B cassette was amplified with primers SacBF-RL13-2 and SacBR-RL13-2 and inserted into the BAC and then removed with oligonucleotide tetO-RL13, leaving behind 1 tet operator. To insert 2 tet operators 33 bp upstream of the UL131A coding region, the *lacZ*/*amp*^{r}/*sac*B cassette was amplified with primers SacBF-UL131A and SacBR-UL131A and inserted into the BAC and then removed with oligonucleotide tetO-UL131A, leaving behind 2 tet operators.

Tagging RL13 in BACs with a V5 epitope. A sequence encoding a V5 epitope was fused to the C terminus of gpRL13 by recombineering. The *lacZ*/*amp*^{r}/*sac*B cassette was amplified with primers SacBF-RL13Hom and SacBR-RL13Hom and inserted after the RL13 ORF within the BAC; then the cassette was removed using overlapping oligos V5-RL13-F and V5-RL13-R, which fused the coding sequence for a V5 tag to the end of gene RL13.

Generating replication-deficient RAd vectors. RL13 was cloned by recombineering into a RAd using the AdZ system as described previously (62), using primers RL13F and RL13R, so that the gpRL13 was tagged with a C-terminal V5 epitope. Virus was recovered from the vector by transfection into 293TREx cells and titrated as described previously (62). Empty vector control (RAd-Ctrl) and RAd-GFP, which expresses eGFP from a version of the HCMV MIE promoter that contains 2 tet operators 10 bp downstream from the TATA box, have been described previously (62).

Protein predictions. N- and O-linked glycosylation sites were predicted using NetNGlyc 1.0 and NetOGlyc 3.1 (87). Signal sequences and transmembrane domains were predicted using SignalP 3.0 (88) and TMHMM 2.0 (http://www.cbs.dtu.dk/services/).

Purification of HCMV virions. HCMV particles in cell supernatants were separated into virion, dense body, and noninfectious enveloped particle (NIEP) fractions by positive density/negative viscosity gradient centrifugation as described previously (89). Particle concentrations in the preparations were estimated by counting negatively stained samples by EM in relation to a standard concentration of latex beads. To separate virion envelope proteins from capsid and tegument proteins, 10^8 particles were mixed 1:1 with envelope stripping buffer (2% Nonidet-P40 in PBS) and incubated for 15 minutes at 4°C. Particles were pelleted (12,000 *g* for 5 minutes at 4°C), and the soluble envelope fraction was harvested. The insoluble capsid/tegument material was washed twice with envelope-stripping buffer and once in PBS before being solubilized in SDS-PAGE sample buffer.

SDS-PAGE and Western immunoblotting. Protein samples were separated by SDS-PAGE using 4%–12% Bis-Tris NuPAGE protein gels (Invitrogen) according to the manufacturer's instructions, then transferred to nitrocellulose by semi-dry transfer. Membranes were blocked overnight in blocking buffer (3% BSA in PBS containing 0.1% Tween 20 [PBST]) and then incubated with primary antibody for 1 hour. Following 3 washes in PBST, secondary antibody was incubated for 1 hour and washed 3 times. Bound antibody was detected using ECL–Western blotting detection system (RPN 2132; Amersham) and exposure to film. Primary antibodies were chicken anti-V5 (9113; Abcam), mouse anti-gB (CMV-023-40154; Capricorn), and mouse anti-pp65 (CMV-018-48151; Capricorn). Secondary antibodies were goat anti–chicken-HRP (6877; Abcam) and goat anti–mouse-HRP (170-6516; Bio-Rad).

Glycosidase treatment. Samples were treated with PNGase F (P0705S; New England BioLabs) or ENDO H (P0703S; New England BioLabs) according to the manufacturer's instructions. Briefly, the samples were denatured in glycoprotein-denaturing buffer at 100°C for 10 minutes and cooled to 0°C for 5 minutes. The samples were then digested overnight at 37°C with PNGase F or ENDO H before being analyzed by Western immunoblotting.

Immunogold electron microscopy. Purified virions were air-dried to the surface of Formvar-coated EM grids. The grids were treated with chicken anti-V5 antibody (9113) for 4 hours at room temperature, washed 3 times with PBS, and incubated with goat anti-chicken antibody (39604; Abcam) conjugated to 6-nm gold particles for 1 hour at room temperature. After further washing in PBS, the grids were negatively stained with phosphotungstic acid and subjected to EM.

Immunofluorescence. Cells were plated on glass coverslips and infected with HCMV. At 7 days PI, the cells were fixed in 4% paraformaldehyde, permeabilized with 0.5% NP-40, and incubated with primary antibody for 1 hour at 37°C. Following washing, secondary antibodies were incubated for 1 hour at 37°C, washed again, and mounted. Primary antibodies were chicken anti-V5 (9113; Abcam), sheep anti-human TGN46 (AHP500; Serotec), mouse MAb anti-pp28 (6502; Abcam), and mouse anti-gH (2470-5437; Biogenesis). Secondary antibodies were donkey anti-chicken Cy3 (AP194C; Millipore), donkey anti-sheep IgG–Alexa Fluor 633 (A21100; Invitrogen), and donkey anti-mouse IgG–Alexa Fluor 488 (A-2102; Invitrogen). The intracellular locations of antibody-tagged proteins were examined under laser illumination in a Zeiss LMS 510 confocal microscope, and images were captured using LMS software.

Statistics. Means ± SD were calculated using GraphPad Prims software.

Acknowledgments

This work was supported by the Wellcome Trust, the United Kingdom Medical Research Council (MRC), and the Biotechnology and Biological Sciences Research Council (BBSRC). The authors thank Sian Llewellyn-Lacey and Carole Rickards for tissue culture support; Brent Ryckman for helpful discussions; Neal Copeland, Dong Yu, and Uta Höpken for reagents; Richard Darley and Phillip Taylor for reagents and advice regarding retrovirus generation; and Jim Aitken for performing the EM.

Received for publication March 12, 2010, and accepted in revised form June 23, 2010.

Address correspondence to: Richard Stanton, Section of Medical Microbiology, Department of Infection, Immunity and Biochemistry, School of Medicine, Cardiff University, Tenovus Building, Heath Park, Cardiff CF14 4XN, United Kingdom. Phone: 44.0.29.20687319; Fax: 44.0.29.20742161; E-mail: StantonRJ@cf.ac.uk.

1. Mocarski ES. Cytomegaloviruses. In: Fields BN, Knipe DM, Howley PM, eds. *Fields Virology*. 5th ed. Philadelphia, Pennsylvania, USA: Lippincott–Raven; 2006:2447–2492.
2. Stratton KR, Durch JS, Lawrence RS. *Vaccines for the 21st Century: A Tool for Decisionmaking*. Washington, DC, USA: National Academies Press; 2000.
3. Sinzger C, Grefte A, Plachter B, Gouw AS, The TH, Jahn G. Fibroblasts, epithelial cells, endothelial cells and smooth muscle cells are major targets of human cytomegalovirus infection in lung and gastrointestinal tissues. *J Gen Virol*. 1995;76(pt 4):741–750.
4. Sinzger C, Plachter B, Grefte A, The TH, Jahn G. Tissue macrophages are infected by human cytomegalovirus in vivo. *J Infect Dis*. 1996;173(1):240–245.
5. Bissinger AL, Sinzger C, Kaiserling E, Jahn G. Human cytomegalovirus as a direct pathogen: correlation of multiorgan involvement and cell distribution with clinical and pathological findings in a case of congenital inclusion disease. *J Med Virol*. 2002;67(2):200–206.
6. Kahl M, Siegel-Axel D, Stenglein S, Jahn G, Sinzger C. Efficient lytic infection of human arterial endothelial cells by human cytomegalovirus strains. *J Virol*. 2000;74(16):7628–7635.
7. Riegler S, Hebart H, Einsele H, Brossart P, Jahn G, Sinzger C. Monocyte-derived dendritic cells are permissive to the complete replicative cycle of human cytomegalovirus. *J Gen Virol*. 2000;81(pt 2):393–399.
8. Quinnan GV Jr, et al. Comparative virulence and

immunogenicity of the Towne strain and a nonattenuated strain of cytomegalovirus. *Ann Intern Med.* 1984;101(4):478–483.
9. Plotkin SA, Starr SE, Friedman HM, Gonczol E, Weibel RE. Protective effects of Towne cytomegalovirus vaccine against low-passage cytomegalovirus administered as a challenge. *J Infect Dis.* 1989;159(5):860–865.
10. Elek SD, Stern H. Development of a vaccine against mental retardation caused by cytomegalovirus infection in utero. *Lancet.* 1974;1(7845):1–5.
11. Cha TA, Tom E, Kemble GW, Duke GM, Mocarski ES, Spaete RR. Human cytomegalovirus clinical isolates carry at least 19 genes not found in laboratory strains. *J Virol.* 1996;70(1):78–83.
12. Prichard MN, Penfold ME, Duke GM, Spaete RR, Kemble GW. A review of genetic differences between limited and extensively passaged human cytomegalovirus strains. *Rev Med Virol.* 2001;11(3):191–200.
13. Davison AJ, et al. The human cytomegalovirus genome revisited: comparison with the chimpanzee cytomegalovirus genome. *J Gen Virol.* 2003; 84(pt 1):17–28.
14. Skaletskaya A, Bartle LM, Chittenden T, McCormick AL, Mocarski ES, Goldmacher VS. A cytomegalovirus-encoded inhibitor of apoptosis that suppresses caspase-8 activation. *Proc Natl Acad Sci U S A.* 2001;98(14):7829–7834.
15. Dargan DJ, Jamieson FE, MacLean J, Dolan A, Addison C, McGeoch DJ. The published DNA sequence of human cytomegalovirus strain AD169 lacks 929 base pairs affecting genes UL42 and UL43. *J Virol.* 1997;71(12):9833–9836.
16. Mocarski ES, Prichard MN, Tan CS, Brown JM. Reassessing the organization of the UL42-UL43 region of the human cytomegalovirus strain AD169 genome. *Virology.* 1997;239(1):169–175.
17. Brown JM, Kaneshima H, Mocarski ES. Dramatic interstrain differences in the replication of human cytomegalovirus in SCID-hu mice. *J Infect Dis.* 1995;171(6):1599–1603.
18. Bradley AJ, et al. High-throughput sequence analysis of variants of human cytomegalovirus strains Towne and AD169. *J Gen Virol.* 2009; 90(pt 10):2375–2380.
19. Penfold ME, et al. Cytomegalovirus encodes a potent alpha chemokine. *Proc Natl Acad Sci U S A.* 1999;96(17):9839–9844.
20. Benedict CA, et al. Cutting edge: a novel viral TNF receptor superfamily member in virulent strains of human cytomegalovirus. *J Immunol.* 1999; 162(12):6967–6970.
21. Wills MR, et al. Human cytomegalovirus encodes an MHC class I-like molecule (UL142) that functions to inhibit NK cell lysis. *J Immunol.* 2005; 175(11):7457–7465.
22. Tomasec P, et al. Downregulation of natural killer cell-activating ligand CD155 by human cytomegalovirus UL141. *Nat Immunol.* 2005;6(2):181–188.
23. Cerboni C, et al. Human cytomegalovirus strain-dependent changes in NK cell recognition of infected fibroblasts. *J Immunol.* 2000;164(9):4775–4782.
24. Goodrum F, Reeves M, Sinclair J, High K, Shenk T. Human cytomegalovirus sequences expressed in latently infected individuals promote a latent infection in vitro. *Blood.* 2007;110(3):937–945.
25. Petrucelli A, Rak M, Grainger L, Goodrum F. Characterization of a novel Golgi apparatus-localized latency determinant encoded by human cytomegalovirus. *J Virol.* 2009;83(11):5615–5629.
26. Akter P, et al. Two novel spliced genes in human cytomegalovirus. *J Gen Virol.* 2003;84(pt 5):1117–1122.
27. Dolan A, et al. Genetic content of wild-type human cytomegalovirus. *J Gen Virol.* 2004; 85(pt 5):1301–1312.
28. Dargan DJ, et al. Sequential mutations associated with adaptation of human cytomegalovirus to growth in cell culture. *J Gen Virol.* 2010;91(pt 6):1535–1546.
29. Chandler SH, Handsfield HH, McDougall JK. Isolation of multiple strains of cytomegalovirus from women attending a clinic for sexually transmitted disease. *J Infect Dis.* 1987;155(4):655–660.
30. Collier AC, Chandler SH, Handsfield HH, Corey L, McDougall JK. Identification of multiple strains of cytomegalovirus in homosexual men. *J Infect Dis.* 1989;159(1):123–126.
31. Spector SA, Hirata KK, Newman TR. Identification of multiple cytomegalovirus strains in homosexual men with acquired immunodeficiency syndrome. *J Infect Dis.* 1984;150(6):953–956.
32. Baldanti F, et al. Coinfection of the immunocompromised but not the immunocompetent host by multiple human cytomegalovirus strains. *Arch Virol.* 1998;143(9):1701–1709.
33. Chou SW. Reactivation and recombination of multiple cytomegalovirus strains from individual organ donors. *J Infect Dis.* 1989;160(1):11–15.
34. Drew WL, Sweet ES, Miner RC, Mocarski ES. Multiple infections by cytomegalovirus in patients with acquired immunodeficiency syndrome: documentation by Southern blot hybridization. *J Infect Dis.* 1984;150(6):952–953.
35. Stanton R, Westmoreland D, Fox JD, Davison AJ, Wilkinson GW. Stability of human cytomegalovirus genotypes in persistently infected renal transplant recipients. *J Med Virol.* 2005;75(1):42–46.
36. Hassan-Walker AF, Okwuadi S, Lee L, Griffiths PD, Emery VC. Sequence variability of the alpha-chemokine UL146 from clinical strains of human cytomegalovirus. *J Med Virol.* 2004;74(4):573–579.
37. Adler B, Scrivano L, Ruzcics Z, Rupp B, Sinzger C, Koszinowski U. Role of human cytomegalovirus UL131A in cell type-specific virus entry and release. *J Gen Virol.* 2006;87(pt 9):2451–2460.
38. Hahn G, et al. Human cytomegalovirus UL131-128 genes are indispensable for virus growth in endothelial cells and virus transfer to leukocytes. *J Virol.* 2004;78(18):10023–10033.
39. Patrone M, Secchi M, Bonaparte E, Milanesi G, Gallina A. Cytomegalovirus UL131-128 products promote gB conformational transition and gB-gH interaction during entry into endothelial cells. *J Virol.* 2007;81(20):11479–11488.
40. Ryckman BJ, Chase MC, Johnson DC. HCMV gH/gL/UL128-131 interferes with virus entry into epithelial cells: Evidence for cell type-specific receptors. *Proc Natl Acad Sci U S A.* 2008;105(37):14118–14123.
41. Ryckman BJ, Jarvis MA, Drummond DD, Nelson JA, Johnson DC. Human cytomegalovirus entry into epithelial and endothelial cells depends on genes UL128 to UL150 and occurs by endocytosis and low-pH fusion. *J Virol.* 2006;80(2):710–722.
42. Ryckman BJ, et al. Characterization of the human cytomegalovirus gH/gL/UL128-131 complex that mediates entry into epithelial and endothelial cells. *J Virol.* 2008;82(1):60–70.
43. Wang D, Shenk T. Human cytomegalovirus UL131 open reading frame is required for epithelial cell tropism. *J Virol.* 2005;79(16):10330–10338.
44. Waldman WJ, Roberts WH, Davis DH, Williams MV, Sedmak DD, Stephens RE. Preservation of natural endothelial cytopathogenicity of cytomegalovirus by propagation in endothelial cells. *Arch Virol.* 1991;117(3–4):143–164.
45. Sinzger C, et al. Modification of human cytomegalovirus tropism through propagation in vitro is associated with changes in the viral genome. *J Gen Virol.* 1999;80(pt 11):2867–2877.
46. Sinzger C, Knapp J, Plachter B, Schmidt K, Jahn G. Quantification of replication of clinical cytomegalovirus isolates in cultured endothelial cells and fibroblasts by a focus expansion assay. *J Virol Methods.* 1997;63(1–2):103–112.
47. MacCormac LP, Grundy JE. Two clinical isolates and the Toledo strain of cytomegalovirus contain endothelial cell tropic variants that are not present in the AD169, Towne, or Davis strains. *J Med Virol.* 1999;57(3):298–307.
48. Grazia Revello M, et al. In vitro selection of human cytomegalovirus variants unable to transfer virus and virus products from infected cells to polymorphonuclear leukocytes and to grow in endothelial cells. *J Gen Virol.* 2001;82(pt 6):1429–1438.
49. Marchini A, Liu H, Zhu H. Human cytomegalovirus with IE-2 (UL122) deleted fails to express early lytic genes. *J Virol.* 2001;75(4):1870–1878.
50. Murphy E, et al. Coding potential of laboratory and clinical strains of human cytomegalovirus. *Proc Natl Acad Sci U S A.* 2003;100(25):14976–14981.
51. Hahn G, Rose D, Wagner M, Rhiel S, McVoy MA. Cloning of the genomes of human cytomegalovirus strains Toledo, TownevarRIT3, and Towne long as BACs and site-directed mutagenesis using a PCR-based technique. *Virology.* 2003;307(1):164–177.
52. Borst EM, Hahn G, Koszinowski UH, Messerle M. Cloning of the human cytomegalovirus (HCMV) genome as an infectious bacterial artificial chromosome in Escherichia coli: a new approach for construction of HCMV mutants. *J Virol.* 1999; 73(10):8320–8329.
53. Yu D, Smith GA, Enquist LW, Shenk T. Construction of a self-excisable bacterial artificial chromosome containing the human cytomegalovirus genome and mutagenesis of the diploid TRL/IRL13 gene. *J Virol.* 2002;76(5):2316–2328.
54. Sinzger C, et al. Cloning and sequencing of a highly productive, endotheliotropic virus strain derived from human cytomegalovirus TB40/E. *J Gen Virol.* 2008;89(pt 2):359–368.
55. Copeland NG, Jenkins NA, Court DL. Recombineering: a powerful new tool for mouse functional genomics. *Nat Rev Genet.* 2001;2(10):769–779.
56. Court DL, Sawitzke JA, Thomason LC. Genetic engineering using homologous recombination. *Annu Rev Genet.* 2002;36:361–388.
57. Smith GA, Enquist LW. A self-recombining bacterial artificial chromosome and its application for analysis of herpesvirus pathogenesis. *Proc Natl Acad Sci U S A.* 2000;97(9):4873–4878.
58. Hobom U, Brune W, Messerle M, Hahn G, Koszinowski UH. Fast screening procedures for random transposon libraries of cloned herpesvirus genomes: mutational analysis of human cytomegalovirus envelope glycoprotein genes. *J Virol.* 2000; 74(17):7720–7729.
59. Cunningham C, et al. Sequences of complete human cytomegalovirus genomes from infected cell cultures and clinical specimens. *J Gen Virol.* 2010; 91(pt 3):605–615.
60. Sanchez V, Clark CL, Yen JY, Dwarakanath R, Spector DH. Viable human cytomegalovirus recombinant virus with an internal deletion of the IE2 86 gene affects late stages of viral replication. *J Virol.* 2002;76(6):2973–2989.
61. Griffin C, et al. Characterization of a highly glycosylated form of the human cytomegalovirus HLA class I homologue gpUL18. *J Gen Virol.* 2005; 86(pt 11):2999–3008.
62. Stanton RJ, McSharry BP, Armstrong M, Tomasec P, Wilkinson GW. Re-engineering adenovirus vector systems to enable high-throughput analyses of gene function. *Biotechniques.* 2008;45(6):659–662, 664–668.
63. Yao F, Svensjo T, Winkler T, Lu M, Eriksson C, Eriksson E. Tetracycline repressor, tetR, rather than the tetR-mammalian cell transcription factor fusion derivatives, regulates inducible gene expression in mammalian cells. *Hum Gene Ther.* 1998;9(13):1939–1950.
64. Lilja AE, Shenk T. Efficient replication of rhesus cytomegalovirus variants in multiple rhesus and human cell types. *Proc Natl Acad Sci U S A.* 2008;105(50):19950–19955.
65. Drake JW, Hwang CB. On the mutation rate of herpes simplex virus type 1. *Genetics.* 2005;170(2):969–970.

66. Bradley AJ, et al. Genotypic analysis of two hypervariable human cytomegalovirus genes. *J Med Virol*. 2008;80(9):1615–1623.
67. Lurain NS, et al. Analysis of the human cytomegalovirus genomic region from UL146 through UL147A reveals sequence hypervariability, genotypic stability, and overlapping transcripts. *Virol J*. 2006;3:4.
68. He R, et al. Sequence variability of human cytomegalovirus UL146 and UL147 genes in low-passage clinical isolates. *Intervirology*. 2006;49(4):215–223.
69. Mattick C, et al. Linkage of human cytomegalovirus glycoprotein gO variant groups identified from worldwide clinical isolates with gN genotypes, implications for disease associations and evidence for N-terminal sites of positive selection. *Virology*. 2004; 318(2):582–597.
70. Rasmussen L, Geissler A, Cowan C, Chase A, Winters M. The genes encoding the gCIII complex of human cytomegalovirus exist in highly diverse combinations in clinical isolates. *J Virol*. 2002;76(21):10841–10848.
71. Rasmussen L, Geissler A, Winters M. Inter- and intragenic variations complicate the molecular epidemiology of human cytomegalovirus. *J Infect Dis*. 2003;187(5):809–819.
72. Davison AJ, et al. Homology between the human cytomegalovirus RL11 gene family and human adenovirus E3 genes. *J Gen Virol*. 2003;84(pt 3):657–663.
73. Sylwester AW, et al. Broadly targeted human cytomegalovirus-specific CD4+ and CD8+ T cells dominate the memory compartments of exposed subjects. *J Exp Med*. 2005;202(5):673–685.
74. Cobbs CS, et al. Human cytomegalovirus infection and expression in human malignant glioma. *Cancer Res*. 2002;62(12):3347–3350.
75. Luo MH, Fortunato EA. Long-term infection and shedding of human cytomegalovirus in T98G glioblastoma cells. *J Virol*. 2007;81(19):10424–10436.
76. Mitchell DA, et al. Sensitive detection of human cytomegalovirus in tumors and peripheral blood of patients diagnosed with glioblastoma. *Neuro Oncol*. 2008;10(1):10–18.
77. Dunn KC, Aotaki-Keen AE, Putkey FR, Hjelmeland LM. ARPE-19, a human retinal pigment epithelial cell line with differentiated properties. *Exp Eye Res*. 1996; 62(2):155–169.
78. Stanton RJ, McSharry BP, Rickards CR, Wang EC, Tomasec P, Wilkinson GW. Cytomegalovirus destruction of focal adhesions revealed in a high throughput Western blot analysis of cellular protein expression. *J Virol*. 2007;81(15):7860–7872.
79. Matrosovich M, Matrosovich T, Garten W, Klenk HD. New low-viscosity overlay medium for viral plaque assays. *Virol J*. 2006;3:63.
80. Shizuya H, et al. Cloning and stable maintenance of 300-kilobase-pair fragments of human DNA in Escherichia coli using an F-factor-based vector. *Proc Natl Acad Sci U S A*. 1992;89(18):8794–8797.
81. Hirt B. Selective extraction of polyoma DNA from infected mouse cell cultures. *J Mol Biol*. 1967; 26(2):365–369.
82. Warming S, Costantino N, Court DL, Jenkins NA, Copeland NG. Simple and highly efficient BAC recombineering using galK selection. *Nucleic Acids Res*. 2005;33(4):e36.
83. Grey F, et al. Identification and characterization of human cytomegalovirus-encoded microRNAs. *J Virol*. 2005;79(18):12095–12099.
84. Mokros T, Rehm A, Droese J, Oppermann M, Lipp M, Hopken UE. Surface expression and endocytosis of the human cytomegalovirus-encoded chemokine receptor US28 is regulated by agonist-independent phosphorylation. *J Biol Chem*. 2002;277(47):45122–45128.
85. Kitamura T, et al. Retrovirus-mediated gene transfer and expression cloning: powerful tools in functional genomics. *Exp Hematol*. 2003;31(11):1007–1014.
86. Kinsella TM, Nolan GP. Episomal vectors rapidly and stably produce high-titer recombinant retrovirus. *Hum Gene Ther*. 1996;7(12):1405–1413.
87. Julenius K, Molgaard A, Gupta R, Brunak S. Prediction, conservation analysis, and structural characterization of mammalian mucin-type O-glycosylation sites. *Glycobiology*. 2005;15(2):153–164.
88. Emanuelsson O, Brunak S, von Heijne G, Nielsen H. Locating proteins in the cell using TargetP, SignalP and related tools. *Nat Protoc*. 2007;2(4):953–971.
89. Irmiere A, Gibson W. Isolation and characterization of a noninfectious virion-like particle released from cells infected with human strains of cytomegalovirus. *Virology*. 1983;130(1):118–133.